2007-07-18

# Seismic and Well Log Attribute Analysis of the Jurassic Entrada/ Curtis Interval Within the North Hill Creek 3D Seismic Survey, Uinta Basin, Utah, A Case History

Ryan J. ONeal
*Brigham Young University - Provo*

# SEISMIC AND WELL LOG ATTRIBUTE ANALYSIS OF THE JURASSIC ENTRADA/CURTIS INTERVAL WITHIN THE NORTH HILL CREEK 3D SEISMIC SURVEY, UINTA BASIN, UTAH, A CASE HISTORY

by

Ryan J. O'Neal

A thesis submitted to the faculty of

Brigham Young University

In partial fulfillment of the requirements for the degree of

Master of Science

Department of Geological Sciences

Brigham Young University

December 2007

BRIGHAM YOUNG UNIVERSITY

GRADUATE COMMITTEE APPROVAL

of a thesis submitted by

Ryan J. O'Neal

This thesis has been read by each member of the following graduate committee and by majority vote has been found to be satisfactory.

| | |
|---|---|
| Date | Thomas H. Morris<br>Chair, Graduate Committee |
| Date | John H. McBride |
| Date | Scott M. Ritter |

BRIGHAM YOUNG UNIVERSITY

As chair of the candidate's graduate committee, I have read the thesis of Ryan J. O'Neal in its final form and have found that (1) its format, citations, and bibliographical styles are consistent and acceptable and fulfill university and department style requirements; (2) its illustrative materials including figures, tables, and charts are in place; and (3) the final manuscript is satisfactory to the graduate committee and is ready for submission to the university library.

_____ _____

Date

Thomas H. Morris
Chair, Graduate Committee

Accepted for the Department

_____

Scott M. Ritter
Department Chair

Accepted for the College

_____

Thomas W. Sederberg
Associate Dean
College of Physical and
Mathematical Sciences

## ABSTRACT

# SEISMIC AND WELL LOG ATTRIBUTE ANALYSIS OF THE JURASSIC ENTRADA/CURTIS INTERVAL WITHIN THE NORTH HILL CREEK 3D SEISMIC SURVEY, UINTA BASIN, UTAH, A CASE HISTORY

Ryan J. O'Neal

Department of Geological Sciences

Master of Science

3D seismic attribute analysis of the Jurassic Entrada/Curtis interval within the North Hill Creek (NHC) survey has been useful in delineating reservoir quality eolian-influenced dune complexes. Amplitude, average reflection strength and spectral decomposition appear to be most useful in locating reservoir quality dune complexes, outlining their geometry and possibly displaying lateral changes in thickness. Cross sectional views displaying toplap features likely indicate an unconformity between Entrada clinoforms below and Curtis planar beds above. This relationship may aid the explorationist in discovering this important seismic interval. Seismic and well log attribute values were cross plotted and have

revealed associations between these data. Cross plots are accompanied by regression lines and $R^2$ values which support our interpretations.

Although reservoir quality dune complexes may be delineated, the Entrada/Curtis play appears to be mainly structural. The best producing wells in the survey are associated with structural or stratigraphic relief and the thickest Entrada/Curtis intervals. Structural and stratigraphic traps are not always associated with laterally extensive dune complexes. Time structure maps as well as isochron maps have proven useful in delineating the thickest and/or gas prone portions of the Entrada/Curtis interval as well as areas with structural and stratigraphic relief. We have observed that the zones of best production are associated with low gamma ray (40-60 API) values. These low values are associated with zones of high amplitude. Thus, max peak amplitude as a seismic attribute may delineate areas of higher sand content (i.e. dune complexes) whereas zones of low amplitude may represent areas of lower sand content (i.e. muddier interdune or tidal flat facies). Lack of significant average porosity does not seem to be related to a lack of production. In fact, the best producing wells have been drilled in Entrada/Curtis intervals where average porosity is near 4 %. There are however zones within the upper portion of the Entrada/Curtis that are 40 ft. (12.2 m) thick and have porosities between 14% and 20%. By combining derived attribute maps with observed cross plot relationships, it appears that the best producing intervals within the Entrada/Curtis are those associated with high amplitudes, API values from 40-60 and structural relief.

**ACKNOWLEDGEMENTS**

I would like to thank Marc Eckels (Vice President of Wind River Resources) for providing Brigham Young University with the North Hill Creek 3D data set. This thesis would not have been possible without your generous contribution. I would like to thank the Utah Geological Survey for their funding of a very large portion of this project. Additional funding was provided by the American Association of Petroleum Geologists and the College of Physical and Mathematical Sciences at Brigham Young University. Software grants from the Landmark (Halliburton) University Grant Program (GeoProbe™, SeisWorks3D™, and ProMAX2D™) and Hampson-Russell were generously donated. I am grateful for the expertise and contributions of R. William Keach II. You made time to answer my many questions even when you didn't have any. To my thesis advisor Dr. Tom Morris, thanks for making it fun and keeping things light hearted. Thank you also to Dr. John McBride and Dr. Scott Ritter for your feedback. Your comments and thoughts have been timely and are appreciated. Most of all, I would like to thank my beautiful wife for her unwavering support in the hardest of times. Your willingness to sacrifice has not gone unnoticed and this would not have been possible without you. To my beautiful daughter, you are the light of my life and have been a constant source of inspiration.

## TABLE OF CONTENTS

LIST OF TABLES



LIST OF FIGURES

## INTRODUCTION

Seismic attribute analysis of the North Hill Creek (NHC) 3D seismic survey is useful in delineating key features of complex Jurassic Entrada/Curtis erg-margin reservoirs. Furthermore, the quantification of these attributes with well log attributes by means of cross plotting has revealed associations between physical rock properties and the seismic data. These associations exist between seismic attributes such as amplitude, reflection strength and energy half-time and well log attributes such as gamma ray values, Entrada/Curtis thickness and porosity. Combining derived attribute maps and seismic/well log attribute cross plots will lead to a better understanding and more efficient exploitation of the Entrada/Curtis Sandstone play in the Uinta basin and to further discoveries in similar erg-margin settings.

Erg-margin sandstones have been recognized as potential stratigraphic and combination traps, especially when they are laterally associated with muddy marine-influenced facies (Vincelette and Chittum, 1981; Fryberger et al., 1983; Fryberger, 1986; Chan, 1989; Mariño and Morris, 1996; Morris et al., 2005; Monn 2006). Gas productive reservoirs of this type have recently been discovered within the North Hill Creek (NHC) 3D seismic survey area and are associated with the Jurassic Entrada/Curtis Sandstone. During the fall of 2002, the high quality, 27 square mile (70 square kilometers) NHC survey was obtained and is located in the southern Uinta basin (Fig. 1). The survey has played an integral part in the discovery and continued development of this Jurassic play.

The NHC survey was the first of its kind in the Uinta basin and led to the drilling of 15 out of 15 successful wells (Fig. 2; Table 1), several of which are among the best gas

producers in Utah. Production is co-mingled with other Mesozoic units although much of the gas is being produced from the Jurassic Entrada/Curtis formations (Fig. 3). Historically, exploration has been focused on Tertiary rocks. The success of the NHC wells has ignited great interest in the Jurassic section in areas adjacent to the NHC survey area. As of 2007, eight additional 3D surveys were acquired in surrounding areas.

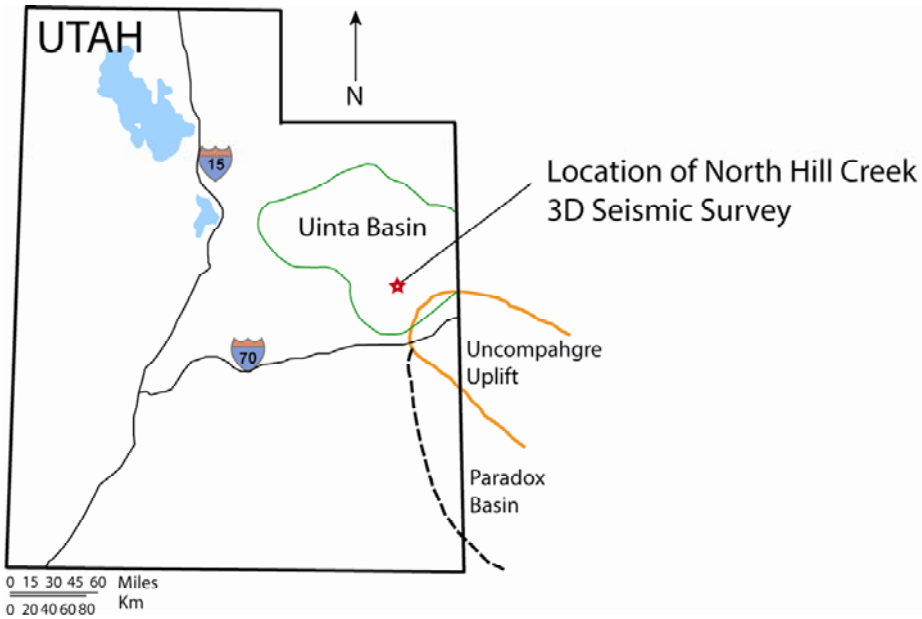


Figure 1: Map showing the location of the North Hill Creek field (NHC). The NHC field geographically overlaps the Flat Rock field.

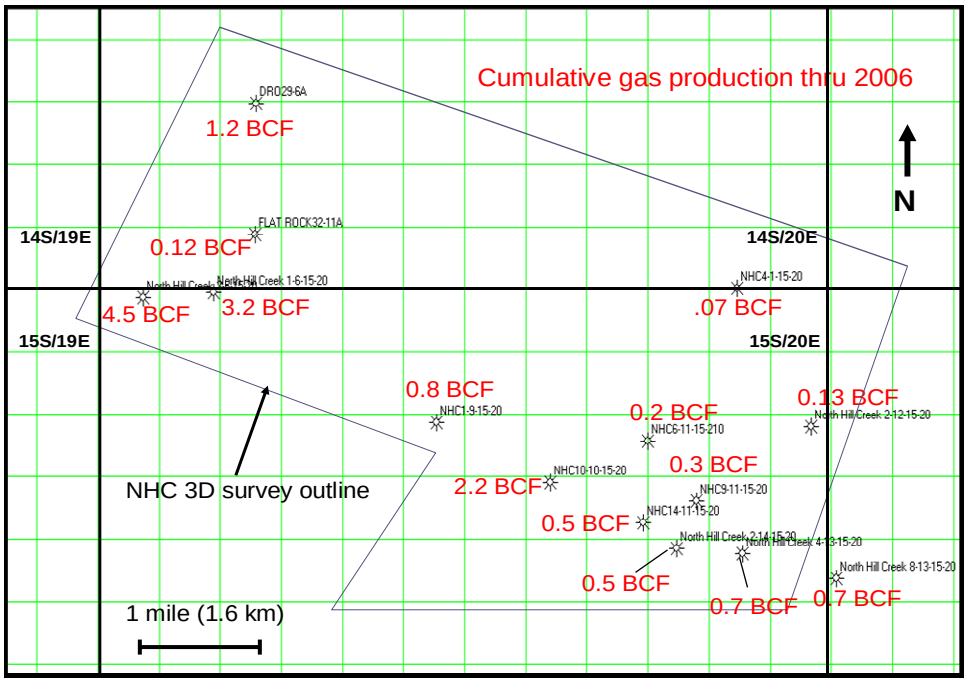


Figure 2: NHC survey outline with 14 of the 15 successful well locations corresponding to Table 1. The area of the NHC survey is approximately 27 square miles. Approximate Township and Range locations are given for orientation.

| | Well | Cumulative Production 2002-2006 |
|---|---|---|
| 1 | NHC 3-6 | 4.5 BCF |
| 2 | NHC 1-6 | 3.2 BCF |
| 3 | NHC 10-10 | 2.2 BCF |
| 4 | DelRio/Orion 29-6A | 1.2 BCF |
| 5 | NHC 1-9 | 0.8 BCF |
| 6 | NHC 4-13 | 0.7 BCF |
| 7 | NHC 8-13 | 0.7 BCF |
| 8 | NHC 14-11 | 0.5 BCF |
| 9 | NHC 2-14 | 0.5 BCF |
| 10 | NHC 9-11 | 0.3 BCF |
| 11 | NHC 6-11 | 0.2 BCF |
| 12 | NHC 2-12 | 0.1 BCF |
| 13 | Flat Rock 32-11A | 0.1 BCF |
| 14 | NHC 4-13 | 0.1 BCF |

Table 1: Cumulative production from 2002 to 2006 for 12 NHC wells and the DelRio/Orion 29-6A and Flat Rock 32-11A wells. Numbers correspond to those in figure 2. All wells penetrate the Entrada/Curtis interval and are located in the NHC survey.

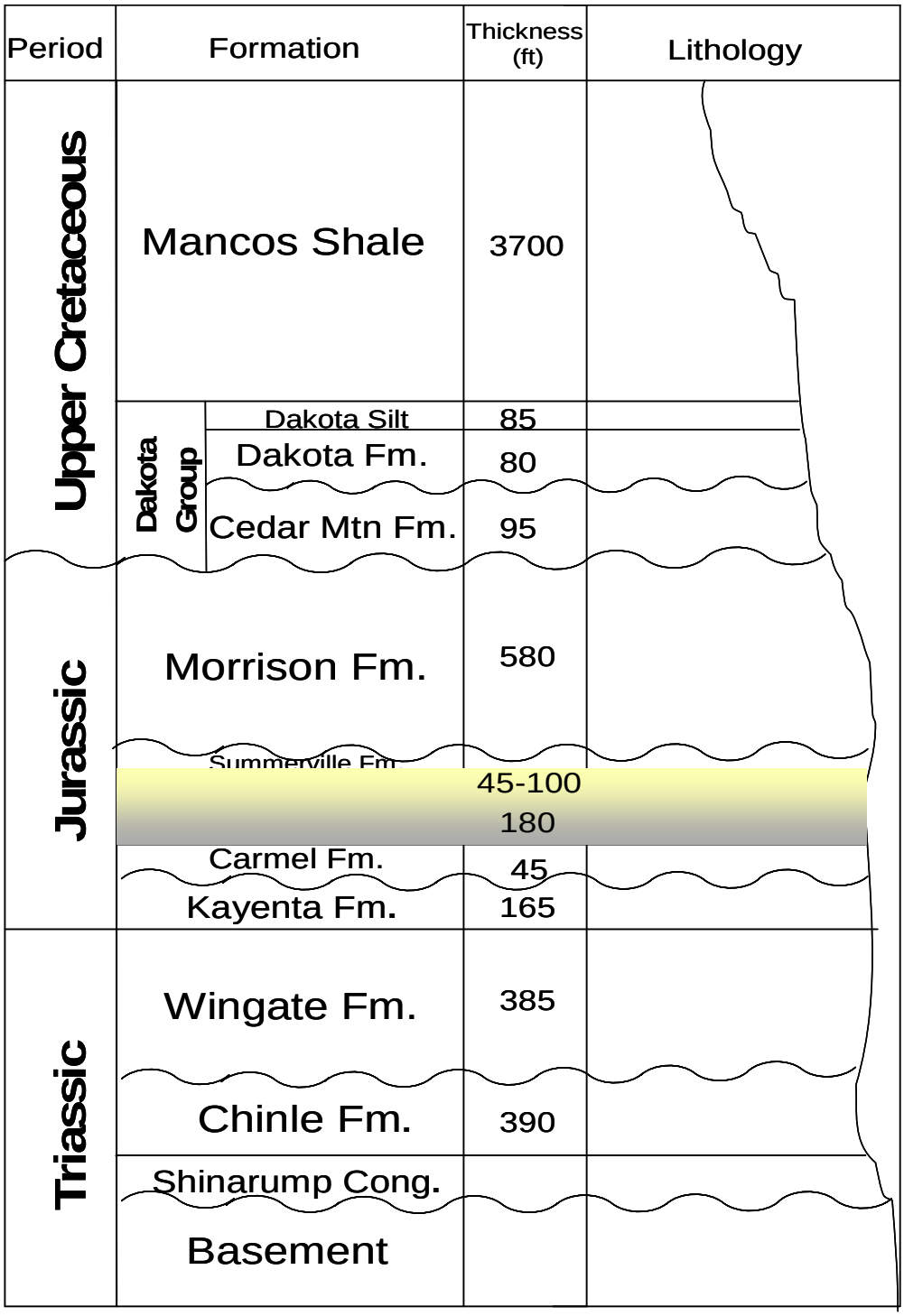


Figure 3: Stratigraphic section within the North Hill Creek field of the Uinta basin (Modified from Eckels et. al., 2005). Stratigraphic interval of interest is the Jurassic Entrada/Curtis section. The Entrada and the Curtis are separated by the J-3 unconformity.

**North Hill Creek 3D Seismic Survey**

The North Hill Creek 3D seismic survey is a 27 square miles (70 square kilometers) survey within the southern Uinta basin. It is located within the Uintah and Ouray Indian Reservation. The survey is the first large-scale exploration-oriented 3D survey acquired in the Uinta basin. It was designed to delineate the structure of a portion of the Hill Creek anticline as well as strata ranging from 2000 ft (609 m) deep Tertiary rocks to the Jurassic section at depths greater than 11,500 ft (3505 m) (Eckels et al., 2006).

A mixed-source design was chosen due to extremely rough terrain in the survey area including a 7,500 ft. (2286 m) elevation mesa bounded and dissected by 1,000 ft. (305 m)deep canyons. The final survey consisted of 81% vibroseis and 19% dynamite shot-hole sources. The source lines were oriented northeast-southwest and spaced at 1,320 ft. (402 m) with source points spaced at 220 ft. (67 m) intervals. Receiver lines were oriented east-west and spaced 660 ft. (201 m) apart with receiver stations every 220 ft. (67 m) Sources were recorded in a ten-line swath with each line containing 108 channels. These parameters provided nominal 45-fold data in 110 ft. (34 m) bins (Eckels et al., 2006).

**Entrada/Curtis Formations**

The Entrada Sandstone was deposited during Upper-Middle Jurassic (Callovian) time as an extensive erg in the western interior of the United States (Blakey et al., 1988). Paleopole positions indicate that the erg was situated between 15 and 25° N latitude, a position conducive for erg development as a trade wind feature in a hot, arid climate (Kocurek, 1981). Erg progradation to the northwest was accompanied by the regional retreat of the Carmel-Twin Creek sea during the Early to Middle Callovian (Imlay, 1980). The erg proper was located in most of Colorado, the eastern portion of Utah, and down into much of Arizona and New Mexico. Muddy tidal flat sediments were deposited to the west of the erg. This lateral relationship between clean erg sands and tidal flat muds is significant as erg-margin sandstones have been recognized as potential stratigraphic and combination hydrocarbon traps (Vincelette and Chittum, 1981; Fryberger et al., 1983; Fryberger, 1986; Chan, 1989; Marino and Morris, 1996; Morris et al., 2005; Monn, 2006). The Entrada erg-margin runs from the southern Uinta basin to south central Utah (Fig. 4). During Entrada deposition, the Sundance Sea lay to the north (Rigby, 1978) while the Mongollan Highlands lay to the south.

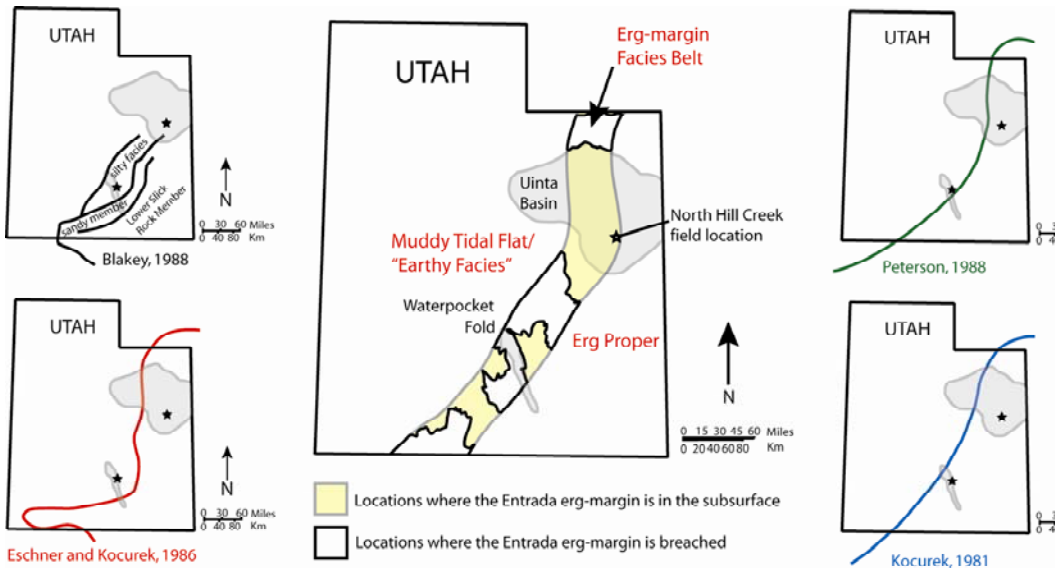


Figure 4: Compilation of past and recent studies delineating the Jurassic Entrada erg-margin. (Modified after Morris et. al., 2005)

The Curtis Formation was deposited as a transgressive systems tract of a complete depositional sequence which included the Middle-Upper Jurassic (Callovian-Oxfordian) Stump and Summerville Formations of Utah and Colorado (Currie et al., 2002). During the transgression of the Curtis Sea from the north, tidal channel deposits of the Curtis Formation began to fill in erosional valleys cut into the underlying Entrada. These valleys were remnants of the regionally extensive J-3 unconformity which developed during a lowstand in sea level. The Curtis Formation grades from west to east from shallow marine and tidal channel deposits to the eolian deposits of the Curtis Moab

Tongue. Petrological studies showthe Curtis Moab Tongue to have exceptional reservoir qualities and this facies is believed to be present within the southern Uinta basin.

The eolian facies of the Moab Tongue was observed near Moab, Utah in contact with the eolian Entrada (Slick Rock Member) which are separated by the J-3 unconformity (Fig. 5). This relationship is significant because the eolian deposits of the Curtis just above the eolian deposits of the Entrada creates a very thick section of high quality reservoir rock. We have observed a similar relationship near Grand Junction, Colorado (Fig. 6) It is likely that both the eolian facies of the Entrada and Curtis are present within the NHC survey area where the Entrada/Curtis interval is between 160-360 ft. (49-110 m) thick.


Figure 5: J3 unconformity candidate at Cottonwood Bend Ranch, east of Moab, Utah on the western flank of the Uncompahgre uplift (looking northwest). Jurassic Curtis Moab Tongue (Jctm)

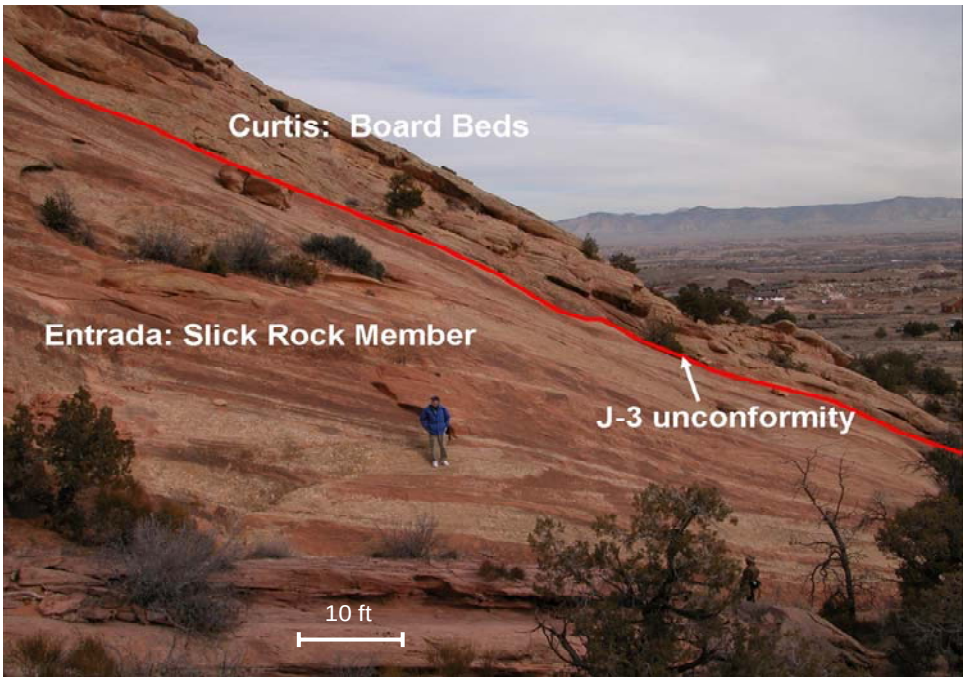


Figure 6: J-3 unconformity near Grand Junction, Colorado on the eastern flank of the Uncompahgre uplift (looking north). Person is standing in bleached foresets of eolian dunes which are interpreted to be "cleaner" sands with higher porosity
than adjacent beds.

The outcrop near Grand Junction differs however from the outcrop near Moab. Instead of large trough cross sets, the Curtis displays planar bedding (dominant) with occasional trough cross sets (Fig. 7). Work to date suggests a depositional environment with a shallow, fluctuating water table due to regional sea level rise as the area transitioned from a wind-dominated regime to a sub-aqueous environment (Potter and Hayden, 2006). The presence of planar beds with occasional trough cross sets near Grand Junction, Colorado argues that the Curtis Sea may have extended along the eastern flank of the Uncompahgre uplift periodically during its existence which in turn reworked existing eolian trough cross sets into planar beds. These re-worked beds also display

massive and horizontal bedding along the north and northwest flanks of the Uncompahgre uplift similar to those described by Vincelette and Chittum (1981) within the upper portion of the Entrada Sandstone in the San Juan basin of New Mexico. Small fluctuations in relative sea level would determine whether dunes prograded seaward or whether shoreline processes reworked existing dunes. This inter-fingering relationship between eolian and shoreface sandstones is likely to be present within the Entrada/Curtis interval of the NHC survey.

Figure 7: Curtis Formation near Grand Junction, Colorado (looking east). Notice the trough cross-stratified facies in between the planar "board beds".

**Entrada/Curtis Contact**

In certain locations, the nature of the J-3 unconformity between the Entrada Sandstone and the Curtis Formation is angular (Fig. 8) (Hintze, 1988; Morris et al., 2005; Monn, 2006). This angular relationship is not always present in either seismic or outcrop. However, where it can be observed seismically, it can definitively clue the interpreter into the Entrada/Curtis-Moab contact. Figure 9 illustrates this relationship in a vertical seismic section, while Figure 10 illustrates a side view of the same line.

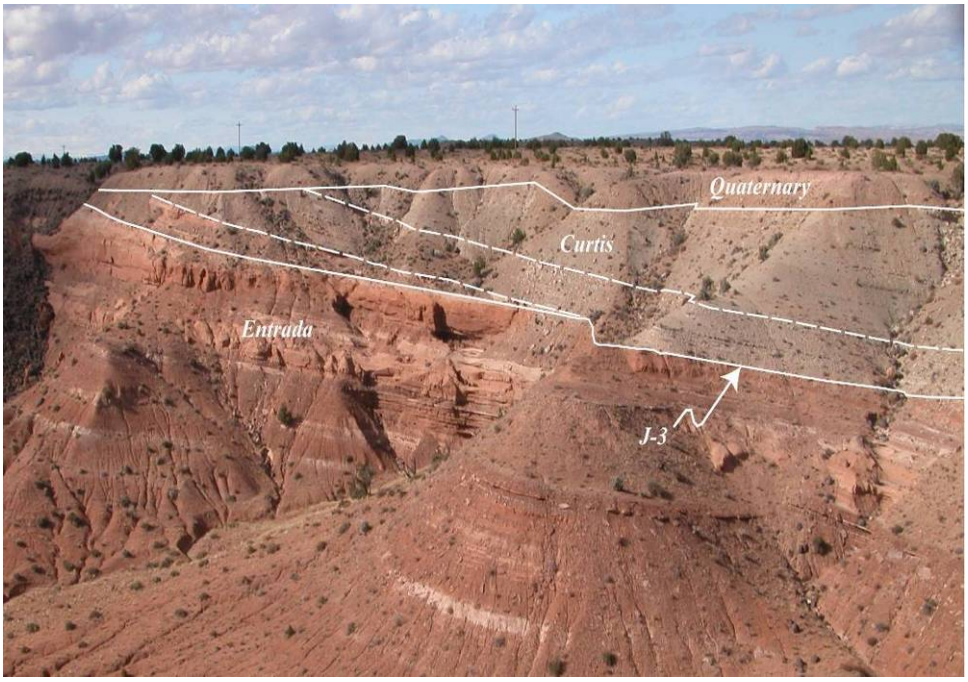


Figure 8: J-3 angular unconformity near Capitol Reef National Park, Utah. This relationship can be found in certain locations but not the whole region. Looking northeast, juniper trees for scale. Notice Curtis downlapping onto Entrada. In other locations the Entrada will toplap into the Curtis.

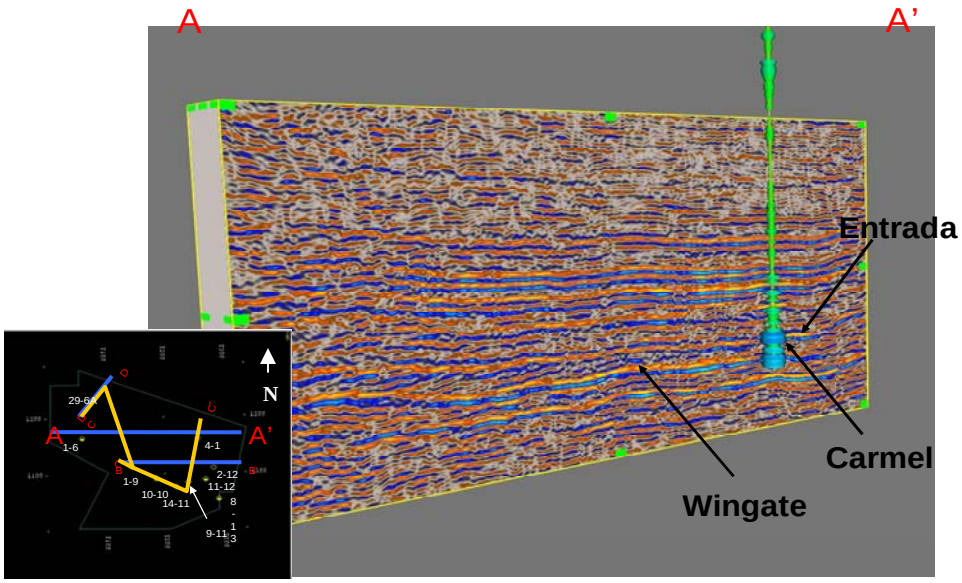


Figure 9: Inline 167 – Note the truncated clinoforms on west end of Entrada seismic interval and apparent stratigraphic thinning over a Wingate structure. Thickness of the Entrada/Curtis interval at well location is 260 ft. A-A' approximately 6 miles. Vertical exaggeration in approximately 10:1. (Modified from Keach et al., 2006)

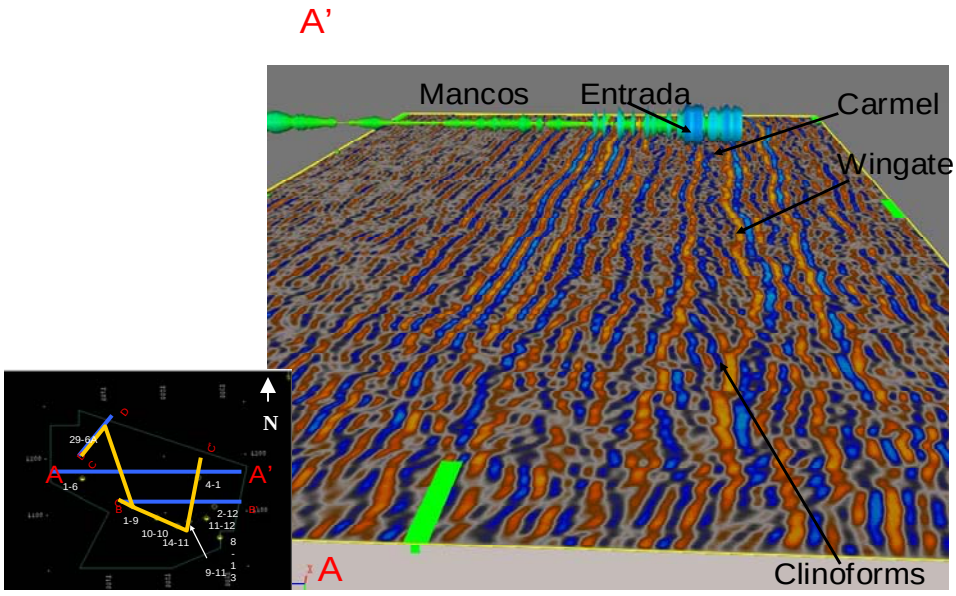


Figure 10: Inline 167 – Line is rotated onto its side to provide another perspective. Note the truncated clinoforms on west end of Entrada/Curtis seismic interval. Thickness of the Entrada/Curtis interval at well location is 260 ft. A-A' approximately 6 miles. Vertical exaggeration in approximately 10:1. (Modified from Keach et al., 2006)

One explanation for the localized angular unconformity at the J-3 is flowage and withdrawal of gypsum within beds of the subjacent Carmel Formation. Diapir-like movement could locally create gentle antiformal folding in the overlying Entrada Sandstone. Gypsum withdrawal in this case may have caused collapse features. Collapsed features within the Entrada can be observed in outcrop on the east flank of the San Rafael Swell. In these locations it appears that the Curtis was unaffected by these collapse features. Thus, the timing of gypsum movement was previous to Curtis deposition.

**Structural Influences**

The Entrada/Curtis Sandstone was deposited on the eastern flanks of the Cordilleran geosyncline. This basin terminated to the southward against the Mogollon uplands and tapered eastward over the craton.

The Uncompahgre uplift played a role in the deposition of erg sands during Entrada time. This uplift was a 31 mi. (50 km) wide NW-SE trending basement-involved arch, bounded on the southwest and northeast by extensive 124-186 mi. (200-300 km) long fault zones that were largely buried by synorogenic and subsequent deposits (Barbeau, 2003) (Fig. 11). Uplift began during the Pennsylvanian and continued until the Middle Permian as part of the Ancestral Rocky Mountain (ARM) orogenic event. The Uncompahgre uplift was reactivated during the Laramide orogeny. The NHC seismic survey is located in the

southern portion of the Uinta basin just to the north of where the structural nose of Uncompahgre uplift plunges into the subsurface. The field itself is cross cut by a NW-SE trending high-angle reverse fault of Laramide age with the hanging wall to the north (Fig. 12). The vertical offset along this fault is approximately 1000 ft. (305 m).

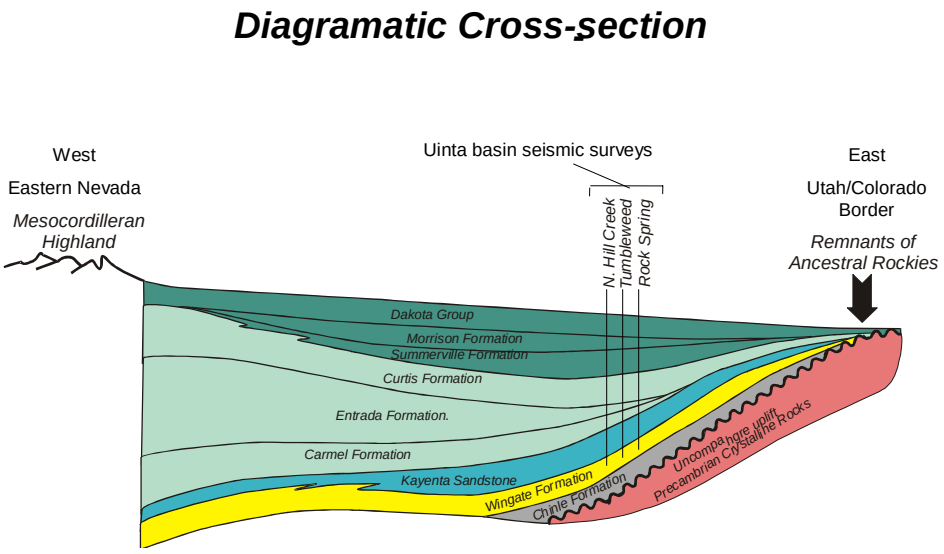


Figure 11: Cross-section of the Jurassic through Precambrian section located south of the Uinta basin. Notice the thinning of strata associated with the Uncompahgre uplift (Modified from Stokes, 1988).

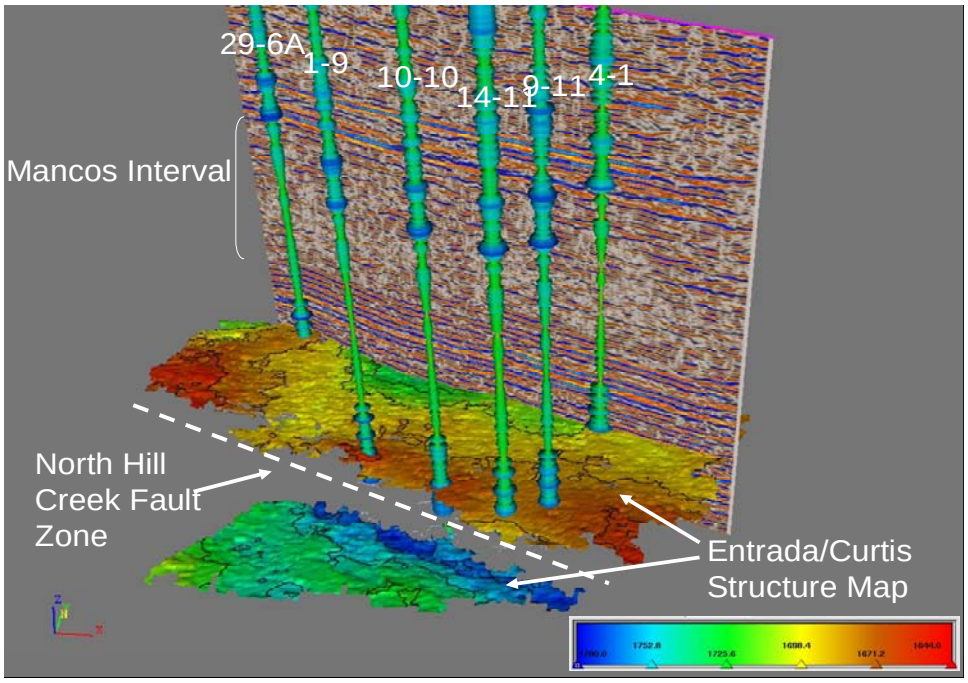


Figure 12: North Hill Creek fault zone. Entrada/Curtis time structure map with gamma ray logs in lathe display. Seismic cross section runs west to east in the northern portion of the survey. Hotter colors represent structural highs while cooler colors represent structural lows. Dashed line approximately 6 miles from left to right. Depth to the top of the Entrada/Curtis interval is approximately 11,000 ft. (3,353 m). Looking northwest (Modified after Keach et al., 2006)

## Entrada/Curtis 3D Seismic Interpretation

Initially, the top of the Entrada/Curtis was mapped as a positive seismic amplitude (Fig. 13).

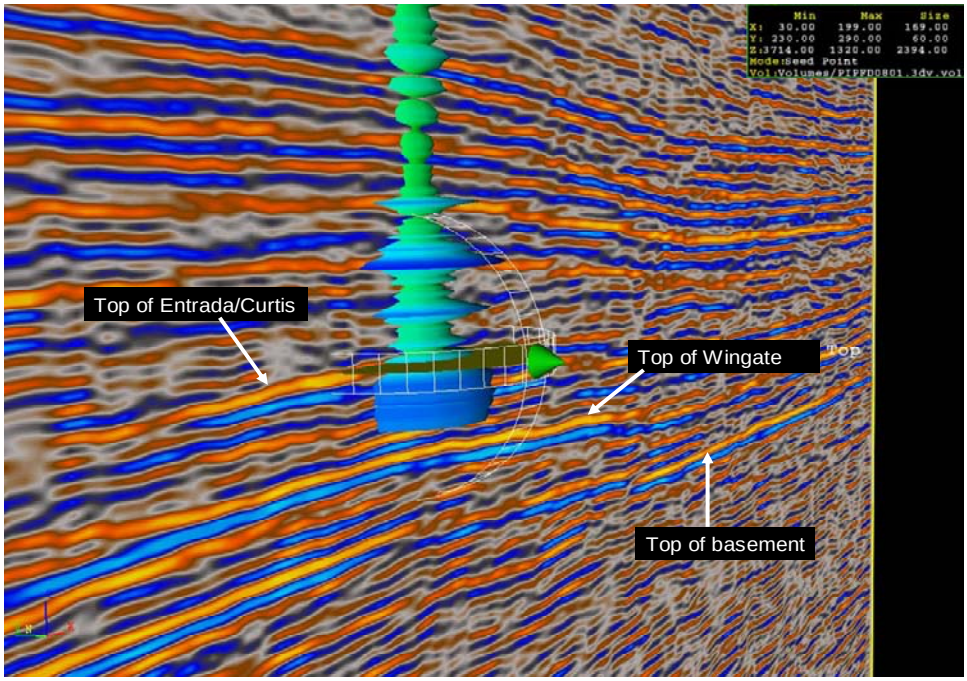


Figure 13: Obique cross section (looking northeast), Seismic peak (orange) with Entrada/Curtis top marker. Del Rio/Orion 29-6A gamma ray log in a lathe display. Blue areas of gamma ray display with large excursions representing lower API numbers. Notice the top of the Wingate and Precambrian basement on the seismic section. These reflectors are key in identifying the Entrada/Curtis interval.

This positive reflector was thought to be caused by the acoustic impedance contrast between the clean gas charged Entrada Sandstone and overlying Summerville which is composed of shale and fine sand. Clinoforms beneath this reflector were also believed to be within the underlying Carmel Formation. Also Precambrian basement is easily identified as the last good reflector as you get deeper in the survey. Based on these

relationships, the peak was easily tracked through most of the survey. However, upon further investigation and generation of synthetic seismograms, we determined that the top of the Entrada/Curtis interval is in fact the trough above our previously mapped peak. This negative amplitude is also easily tracked through most of the survey and is present as a result of the very porous gas charged zone within the Curtis or upper Entrada. Well logs indicate that the upper Entrada/Curtis is defined by a low density, low sonic velocity zone (Fig. 14).

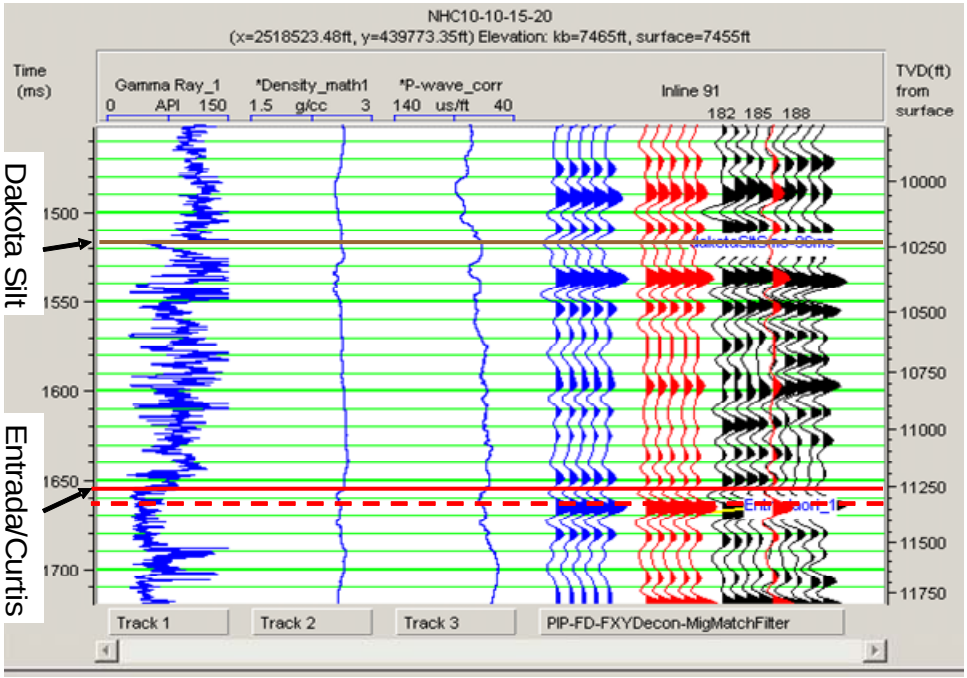


Figure 14: NHC 10-10. Track 1: gamma ray log, track 2: density log (edited), track 3: p-wave sonic log (edited). The synthetic seismogram trace is in blue, the composite trace is in red and the poststack seismic data is in black. Notice the tie between the top of the Entrada/Curtis, the low density/low velocity zone and the poststack seismic trough. The previously mapped peak is the dotted yellow line while the better tie is represented by the solid yellow line.

The mapped seismic peak may be a side lobe of the above trough. This fact however should not affect the validity of the extracted attributes in this study since a 6 millisecond (ms) window was included above the mapped peak. This 6ms window is large enough to include all of the Entrada/Curtis above our mapped seismic peak.

Below the Entrada/Curtis seismic reflector, are two additional peaks that are easily tracked throughout the survey. These two peaks represent the underlying Triassic Wingate Sandstone and Precambrian basement (Fig. 13). Assuming the Entrada/Curtis geometry is similar in surrounding areas, this relationship should make the future picking of the Entrada seismic reflector in nearby seismic surveys relatively easy.

In at least one location within the survey, there is a split in the seismic reflector where the Entrada/Curtis is anomalously thick and associated with a max peak amplitude anomaly (Fig. 15). This increase in thickness likely represents a lack of erosion of the Entrada during sea level lowstand, or an anomalously thick section of Curtis above the Entrada. Kocurek (2000) noted a similar geometry among the Entrada and overlying Todilto Formation near Ghost Ranch in the San Juan basin of New Mexico. The relief in the Entrada was interpreted as having been preserved due to catastrophic flooding of the erg by a sea from the south.

The flat nature of the reflectors immediately beneath the Entrada/Curtis Moab seismic pick, which are located in an otherwise dipping environment, causes one to consider the possibility of a gas/water contact. This anomaly has been drilled and has yielded very good gas production (1.2 BCF).

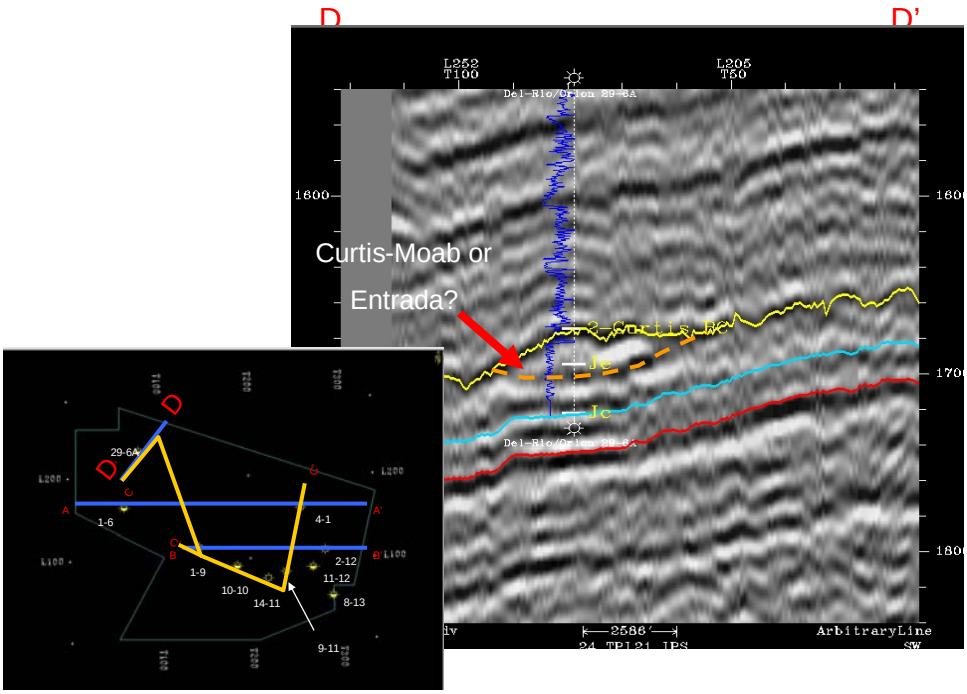


Figure 15: Arbitrary line through DelRio/Orion 29-6A: Entrada horizon, gamma ray log and seismic character shown. Notice the thick section of sand from the gamma ray log (nearly 250ft). The addition of a thick Curtis section may provide greater reservoir volume and a stratigraphic trap.

## Seismic Attributes – An Introduction

Included within this document are numerous seismic images and maps extracted from the North Hill Creek (NHC) 3D seismic survey. These seismic extractions include maximum peak amplitude, average reflection strength, energy half-time, dominant frequency, average instantaneous phase, semblance, and spectral decomposition. We herein provide an introduction as to what these extractions are and what they can potentially produce in helping interpret and understand the Entrada/Curtis interval.

The primary references for this introduction to seismic attributes section comes from: *PostStack Family Reference Manual* copyright © 2004 by Landmark Graphics Corporation.

A suite of seismic attribute computation tools for 2D and 3D seismic data sets was used for this project. The use of seismic attribute analysis for seismic interpretation was first described in the context of seismic sequence analysis (Mitchum et al., 1977). The basic concept of seismic attribute analysis was outlined by Taner and Sheriff (1977). The concept is based on a set of quantitatively derived measures of a seismic waveform that can be used to improve the visual ability of an interpreter to: correlate stratal reflection patterns, recognize distinctive packages of reflections with a similar character, interpret subtle bedding patterns, recognize subtle faults and other geologic features of a seismic section.

The application of seismic attribute analysis to the North Hill Creek 3D seismic survey will (1) improve the general stratigraphic and structural interpretability of the data for the Entrada/Curtis section, (2) create a consistent and quantitative basis for comparing the continuity and coherency of reflections at various levels within the section, and (3) allow us to develop a set of pattern recognition criteria for indicating discontinuities.

**Amplitude**

By analyzing the amplitude- and phase-related interference phenomena, one can quickly and efficiently quantify and map local rock mass variability within a 3D survey.

In general, amplitude information can be useful in identifying:

- gas and fluid accumulation
- gross lithology
- gross porosity
- channel and deltaic sands
- certain types of reefs
- unconformities
- tuning effects
- changing sequence stratigraphy.

Lateral changes in amplitude have been used in stratigraphic studies to separate areas of concordant stratigraphy from chaotic or mounded beds in an interval (Fig. 16). In general, beds that are concordant will have higher maximum amplitudes. Hummocky beds will have lower maximum amplitudes, and chaotic beds, the lowest. In certain Tertiary basins, deltaic sequences prograde from sand-rich shoreline facies to shale-rich pro-delta or abyssal plane facies. Sand-rich environments often have high seismic amplitudes as indicators. Likewise, shale-rich environments often have low seismic amplitudes as indicators. These changes in the sand-shale ratio are readily detected by viewing amplitude statistics in map view. Relative to this study, two possible scenarios exist that may make amplitude extractions helpful. First, amplitude may be used in detecting where sandy erg or erg-margin facies transition laterally to muddy intertidal facies. Second, amplitude extraction may help in detecting where sand-prone dune complexes transition laterally into finer grained interdune facies.

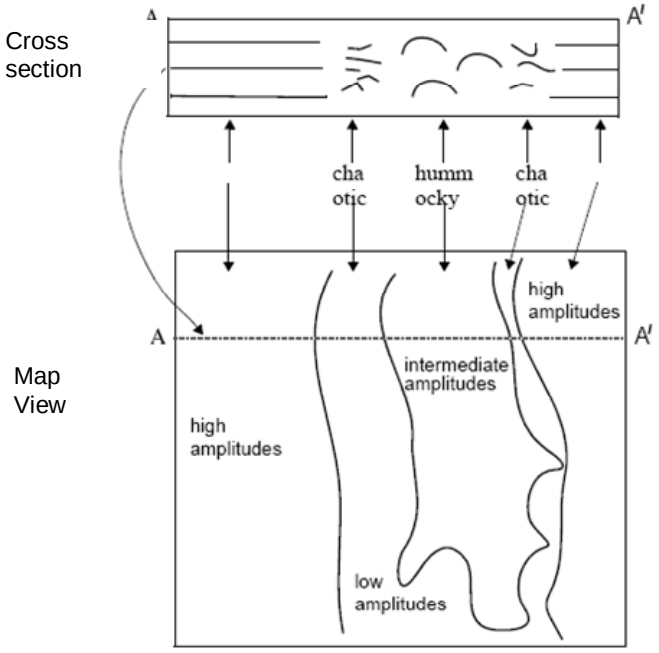


Figure 16: Amplitude as an indicator of stratigraphy. An idealized example of mapping amplitude variations.

**Average Reflection Strength**

Reflection strength is amplitude independent of phase. It is the envelope of the seismic trace. For each time sample, reflection strength is calculated as follows:

$$\text{Reflection strength} = ((\text{real trace})^2 + (\text{quadrature trace})^2)^{1/2}$$

Therefore, reflection strength is always positive and always in the same order of magnitude as the real trace data. In order to calculate the average reflection strength , PAL converts each incoming trace to reflection strength and then computes its mean value. High reflection strength is often associated with major lithologic changes or with gas accumulations.

Average reflection strength has similar application to many amplitude statistics. Average reflection strength however is more sensitive to amplitude anomalies in that it is independent of phase. Average reflection strength may be useful in identifying:

- Changes in sequence amplitudes due to changing lithology or stratigraphy
- Amplitude anomalies due to gas and fluid accumulations, Unconformityes and tuning effects.

In certain Tertiary basins, where sand-rich, shoreward facies grade in to shale-rich basinward facies, average reflection strength has proven to be useful in identifying zones of contrasting sand-shale ratios. This attribute may be useful in identifying lateral changes in the NHC area where erg sands grade laterally into tidal flat and interdune facies.

**Energy Half-Time**

This process computes the energy half-time or the proportion of time required for the energy contained within a time interval to build up to one-half of the total energy contained within the entire interval. In other words, energy half-time allows the interpreter to view how the energy is distributed within his or her zone of interest. Energy half-time values are from 1 to 100. This range of numbers represents the percentage of the window for half of the energy to be dispersed. For example, if we analyzed a window of 100 ms in length, and half of the energy was dispersed in the first

10 ms then the value would be 10. Energy half-time may be useful in identifying lateral discontinuity caused by:

- facies and lithology changes
- changes in porosity
- cementation fronts
- hydrocarbon accumulation

This seismic attribute may be useful in identifying lateral facies changes in the NHC area as well as zones of high porosity in the upper portion of the Entrada/Curtis interval.

**Dominant Frequency**

Instantaneous dominant frequency $f_d(t)$ is defined as the square root of the sum of the squares of the instantaneous frequency f(t) and the instantaneous bandwidth σ(t).

$$fd(t) = ( f^2(t) + \sigma^2(t) )^{1/2}$$

Dominant frequency has units of Hertz with values that range from 0 to Nyquist frequency and occasionally larger. It is always positive and at least as large as instantaneous frequency. Instantaneous dominant frequency is used as a replacement for instantaneous frequency, because it is less susceptible to the problem of spikes and a better measure for tracking reflection spacing. Determining the dominant frequency of the Entrada/Curtis interval in the NHC area may be useful in that it provides future explorationists doing seismic attribute work a parameter that may relate to their study.

**Phase**

Instantaneous phase describes the angle between the phasor, which is a rotating vector formed by the real and imaginary components of the time-series, and the real axis as a function of time. Therefore, it is always a number between -180 and +180 degrees. As a result, instantaneous phase has a discontinuous, sawtooth character caused by the phase-wrapping between +180° to -180° (White, 1991). This character can be corrected by wrapping phase. Analysis window size is important and should be small, typically only a period or less. Each incoming trace is converted into instantaneous phase and then its mean value is computed within the analysis window.

Because phase is sensitive to subtle perturbations in the seismic character, it is ideal for detecting lateral acoustic discontinuities often found in faulted/compartmentalized reservoirs or in areas of lateral facies changes. That is to say, if the rock mass within the analysis window is laterally stable, its phase response will likewise be stable. If a lateral discontinuity occurs, the phase response becomes unstable across the discontinuity. Once the rock mass stabilizes on the other side of the discontinuity the phase response likewise stabilizes.

Average instantaneous phase provides a means of assessing the overall phase characteristics of a seismic interval. Lateral changes in phase may be related to changing fluid content of sediments or even to changes in bedding character within a sequence.

Instantaneous phase should respond in a diagnostic way to amplitude tuning effects. In other words, when amplitude attributes are biased by the constructive and then destructive interference of reflectors as they come closer together, instantaneous phase can confirm that the amplitude changes are due to tuning and not to hydrocarbons or other effects.

**Semblance or Event Similarity Prediction (ESP)**

3-D seismic data are generally binned into a regular grid. By calculating localized waveform similarity in both in-line and cross-line directions, estimates of 3-D seismic coherence are obtained (Bahorich and Farmer, 1995). Event Similarity Prediction (ESP) is Landmark's version of Semblance, coherence or dissimilarity processing. This process, much like coherence, examines the dissimilarity of an event along one trace with the same event along the adjacent trace. The advantage of dissimilarity data is that it reveals and heightens lateral seismic changes that often relate to geologic changes. These dissimilarity measurements yield the visual identification of such features as faults, facies changes, and other geologic patterns. Faults and stratigraphic changes will often stand out as prominent anomalies in otherwise homogenous data. Low similarity values may be caused by the following:

- near vertical faults or low-angle faults
- contrasts in seismic character due to stratigraphic or lithologic changes
- highly dipping events, if dip correction has not been applied

• lack of reflectors (e.g. salt)

• poor quality data

Faulting with detectable vertical throw or wavefield distortion will generally produce clearly identifiable, narrow zones of low similarity. Similarly, abrupt contrasts in seismic character due to stratigraphic or lithologic changes (such as channel sands) will also produce narrow zones of low similarity values.

Gradual stratigraphic contrasts, such as those associated with transgressive sequences, will produce broad regions of moderate similarity values. Highly dipping events, when no dip correction is applied, will result in broad regions of low similarity. Zones with poor data quality or lack of reflectors (e.g. salt structures) can also produce broad regions of low similarity. Finally, bad traces, migration "smiles," and acquisition "foot print" can also generate localized regions of low similarity.

**Spectral Decomposition**

Spectral decomposition is used for imaging and mapping temporal bed thickness and geologic discontinuities over 3D surveys. By transforming the seismic data into the frequency domain via the Discrete Fourier Transform (DFT) (Heideman et al., 1985) the amplitude spectra delineate temporal bed thickness variability while the phase spectra indicate lateral geologic discontinuities. This signal analysis technology has been used successfully in 3-D seismic surveys to delineate stratigraphic settings such as channel sands and structural settings involving complex fault systems. This technology can improve prospect

definition beyond seismic tuning resolution and it can often help resolve what cannot be resolved in the time domain (Partyka et al., 1999). Spectral decomposition is a must use tool for:

- •delineating facies/stratigraphic settings (such as eolian bedform thickness variation, floodplain boundaries, reef boundaries, channel sands, incised valley-fill sands, and other thin beds)
- •resolving the order of deposition
- •detailed mapping of structural settings involving complex fault systems (such as reservoir compartmentalization)
- •mapping of near surface environmental hazards (such as expulsion features and other near surface instabilities)
- •reservoir modeling (mapping fluid changes, pressure changes and changes in 4D surveys).

The frequency slice, also called a "tuning map," is very useful because it provides visualization of thin-bed interference patterns in plan view. Drawing on experience, these tuning maps can be used to identify textures and patterns indicative of geologic processes. Animating through frequency subbands/tuning maps of the earth provides the capability to map lateral variability in the subsurface. However, the interpreter cannot collapse all the information gained by animating through a tuning cube into a single attribute map.

Spectral decomposition can be used qualitatively to reveal stratigraphic and structural edges/bodies as well as relative thickening/thinning. Quantitative use of spectral decomposition is effective at predicting reservoir thickness or intra-reservoir travel time. Whether qualitative or quantitative, spectral decomposition maps usually exhibit substantially more fidelity than full-bandwidth conventional complex trace attributes. Very rarely will the interpreter find information in conventional attributes that is unique to spectral decomposition analysis. That is to say, if the interpreter does not see an event with spectral decomposition, then he/she will not see it with traditional complex trace attributes. Furthermore, events are almost always brighter with spectral decomposition than with traditional attributes. According to most users, when compared to coherency imaging, the spectral decomposition fault definition is often superior. The current study uses spectral decomposition in a qualitative and quantitative approach.

**Isochron Map**

One very common and useful map is the isochron map. Isochron maps display time thickness values as a result of subtracting one mapped seismic event from another. These values can then be displayed in a variety of color bars. Using color to display these maps can reveal key geologic relationships such as depocenter position relative to faulting and zones of high net pay and low net pay. Isochron maps may also be useful in high-grading drilling prospects as thicker sand intervals may easily be identified.

## Seismic Attribute Extraction Parameters

Interpretation of seismic attributes can be quite ambiguous without a foreknowledge of the geologic setting, With a geologic model in mind one can gather useful information from the seismic data. Initially, numerous time windows ranging from 15-45 ms were analyzed and attributes were extracted. A 28 ms window appears to yield the greatest amount of detail in the attribute extraction maps. Also, throughout the North Hill Creek (NHC) survey, the Entrada/Curtis is commonly constrained to a particular time window and we have found this time to be approximately 25 ms +/- a few ms. Thus, our intent in choosing a seismic window is to ensure inclusion of the entire Entrada interval.

**Maximum Peak Amplitude, Average Reflection Strength, Energy Half-Time, Dominant Frequency, Average Instantaneous Phase**

A 28 ms window was chosen which included 6 ms above and 22 ms below our interpreted Entrada/Curtis horizon (top of Entrada/Curtis interval). Maximum peak amplitude, average reflection strength, energy half-time, dominant frequency and average instantaneous phase were extracted from this window and displayed in the appropriate color schemes. These color schemes were chosen at our discretion and in our opinion are the most appropriate for displaying the data.

**Semblance (ESP)**

A semblance volume was calculated on the 3D reflection volume with a 24 ms window from the top of the Entrada/Curtis interval and a 3 trace cross correlation. The semblance values displayed in map view were extracted at 10 ms below the Entrada seismic pick.

**Spectral Decomposition**

The analysis window length for calculation is 40 ms. Spectral decomposition extractions often see slightly larger windows for data analysis. Providing a slightly larger analysis window seems to provide more meaningful maps. A cosine taper of 20% helps to focus on the middle portion of the Entrada seismic interval. The window was centered 10 ms below the Entrada seismic pick. The calculated tuning volume contains frequency slices from 0 Hz to 100 Hz but only 20 Hz, 35 Hz and 50 Hz frequency slices are considered here. These frequency slices have proven to be the most useful in a qualitative sense. When these derived extraction maps are viewed in succession one can generally observe lateral changes in dune complex morphology.

**Isochron Map**

An Entrada/Curtis isochron map was constructed by mapping the Entrada/Curtis interval and subtracting these time values from the time values of a mapped Carmel Formation horizon. The Carmel Formation lies stratigraphically below the Entrada and

should thus give time thickness values for the Entrada/Curtis interval if we subtract one from the other. One problem that becomes quickly apparent when mapping the Carmel horizon is that a laterally extensive seismic event that represents the Carmel top does not exist. This may be due to extensive evaporite movement within the Carmel or simply because the Carmel throughout much of the survey is below tuning thickness. This causes the interpreter to guess on where to make the seismic pick. We understand that this may cause inaccuracy in the calculated isochron map, but we feel confident that the generated map gives the interpreter a good idea of lateral thickness variations. We also have the luxury of having 15 wells drilled in the NHC survey area. The thickness values of the Entrada/Curtis extracted from the well log data match the derived isochron map.

## Seismic Attribute Interpretation

Qualitative seismic attribute interpretations are discussed within this section. The above mentioned attributes were extracted within their respective windows and then assigned color schemes that best display the data. An interpretation is presented for a given 3D seismic attribute and the corresponding map pointing out key zones of interest is shown just below it. Seismic maps in all figures outline the 27 square mile NHC survey.

### Maximum Peak Amplitude

Maximum positive amplitudes are found in the upper portion of the 28 ms. window investigated (Fig. 17). Numerous geologic features are apparent on the

maximum amplitude map, some of which were previously interpreted and described by Eckels et al. (2005). Geologic features interpreted to be visible include star dune complexes, barchan dunes, and longitudinal to sinuous, seif-like dunes. The figure also illustrates that a concentration of star dune complexes can be observed in the southeast third of the 3D survey with scattered complexes in the northwest third of the survey. There appears to be few star dune complexes in the middle of the survey. Gray areas likely represent muddy interdune or tidal flat deposits. Higher amplitudes represented by yellows and reds likely represent the general area of highest sand accumulation but do not necessarily reflect sandstone thickness or reservoir quality. Spectral decomposition may better delineate the thickness of sandstone accumulations.

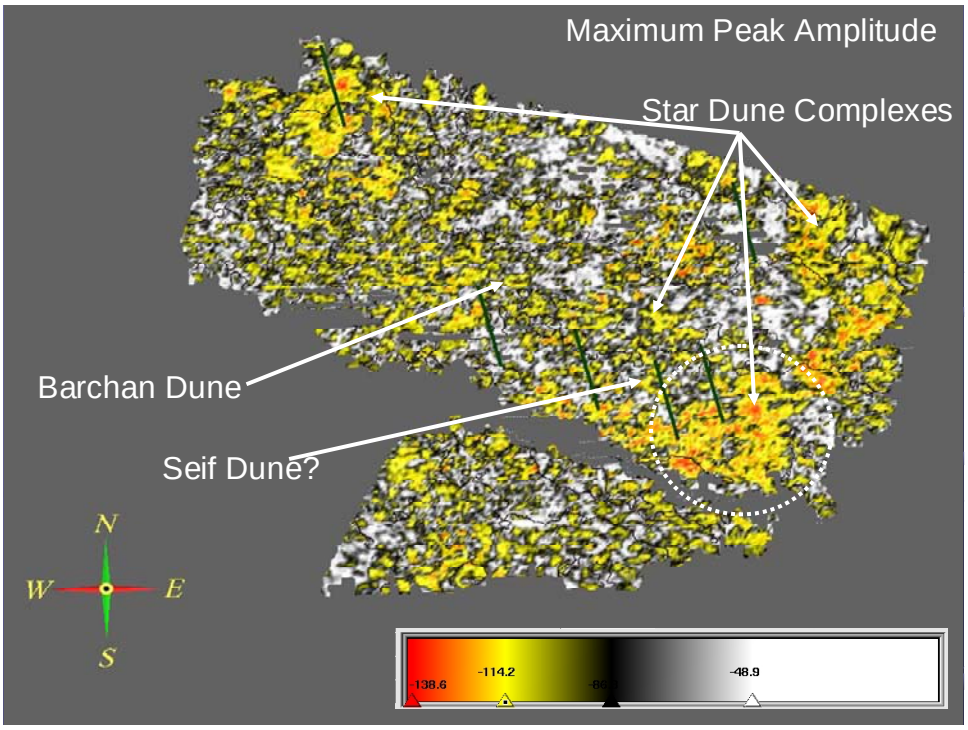


Figure 17: Maximum positive amplitude extraction map for a 28ms window around the Entrada/Curtis interval. Yellows and reds represent the highest peak amplitude while the whites and grays represent the lowest peak amplitudes. (Modified after Keach et. al. 2006)

**Average Reflection Strength**

Average reflection strength appears to show many geologic features that are similar to those shown by maximum peak amplitude (Fig. 18). Star dune complexes are very apparent while the seif and barchanoid structures are less obvious. Average reflection strength does appear, however, to show distinct changes in facies. Erg-margin sandstones are displayed in oranges and yellows while interdune and/or tidal flat facies are displayed in blue. These facies changes are very apparent with the particular color bar we have chosen. Star dune complexes appear to be much more prevalent in the eastern portion of the survey.

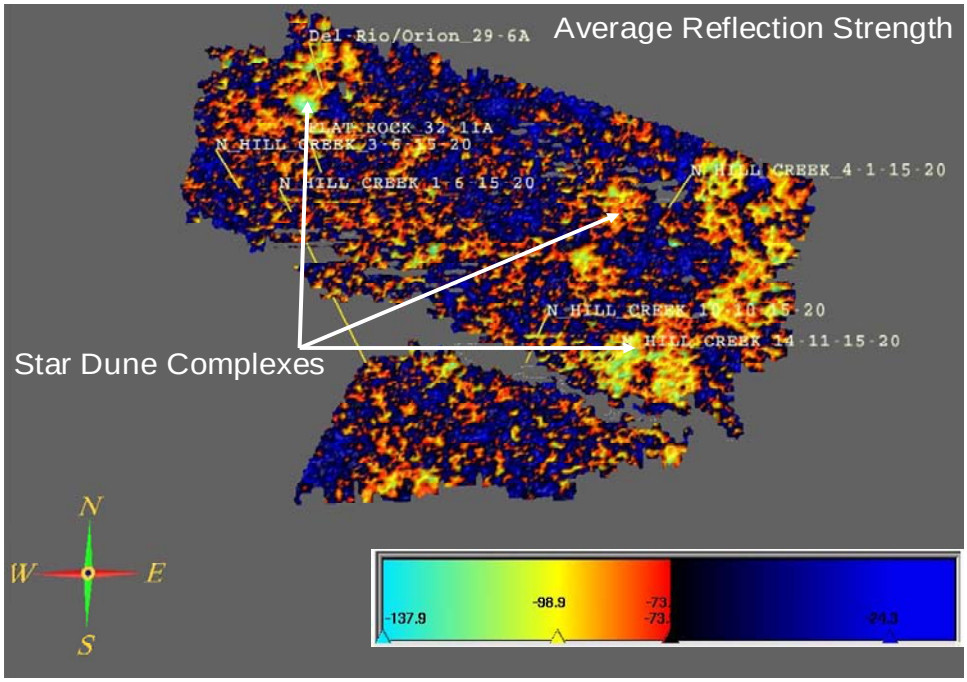


Figure 18: Average reflection strength extraction map for a 28 ms window around the Entrada/Curtis interval. Oranges and yellows represent the zones with the highest average reflection strength while the blues represent zones with lower average reflection strength. Compare to the maximum peak amplitude extraction map.

**Energy Half-Time**

Energy half-time appears to be useful in delineating zones of high energy attenuation in the upper portion of the Entrada/Curtis interval (Fig. 19). These changes may be related to relatively thick sections of high porosity or gas charged zones within the upper portion of the Entrada/Curtis interval (Fig. 20). These zones generally correlate with maximum peak amplitude and average reflection strength maps but the anomalies are not nearly as laterally continuous.

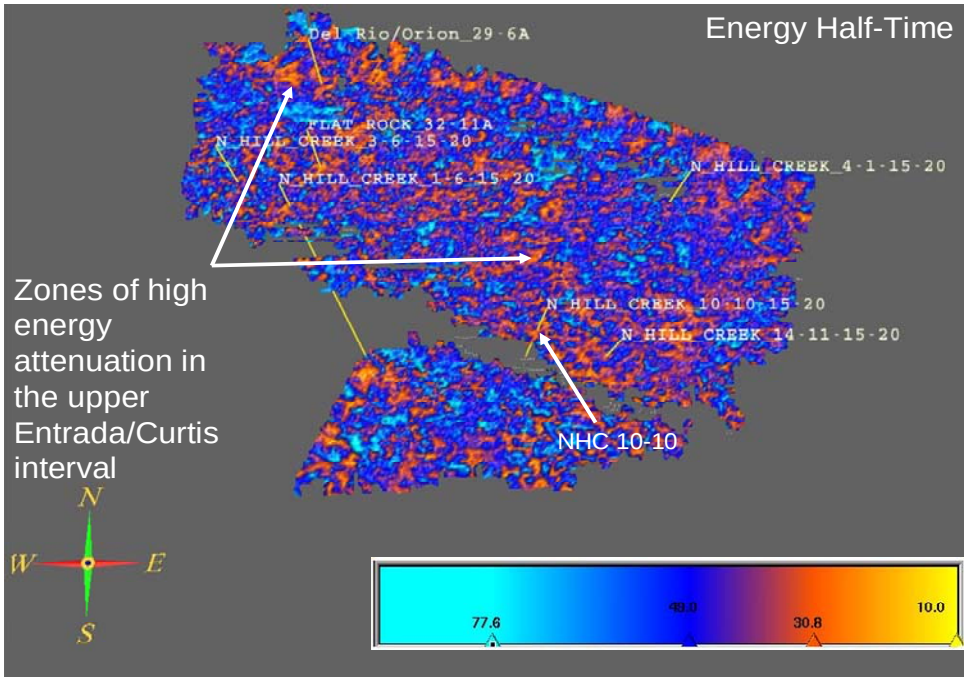


Figure 19: Energy half-time attribute map for a 28 ms window around the Entrada/Curtis interval. Hotter colors represent areas were energy is attenuated very fast in the upper portion of the Entrada/Curtis. Cooler colors represent where energy attenuates much more gradually.

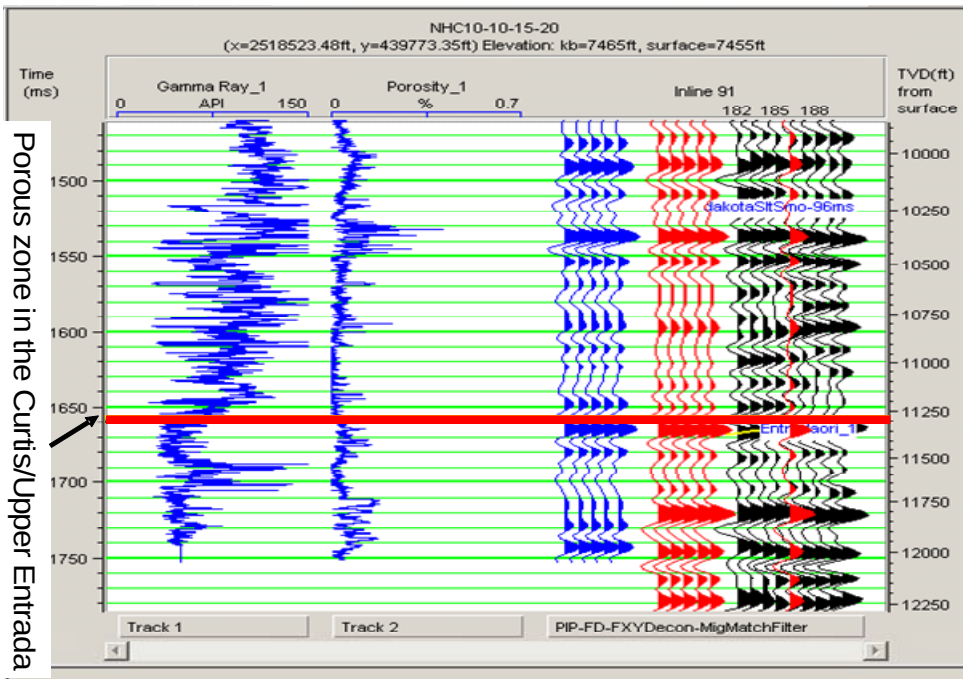


Figure 20: NHC well 10-10. Porous zone within the upper portion of the Entrada/Curtis (red line). It is possible that high energy half-time values are related to these porous zones (Fig. 20).

**Dominant Frequency**

The dominant frequency of the seismic data within the Entrada/Curtis interval appears to range from 30Hz to 40Hz (Fig. 21).

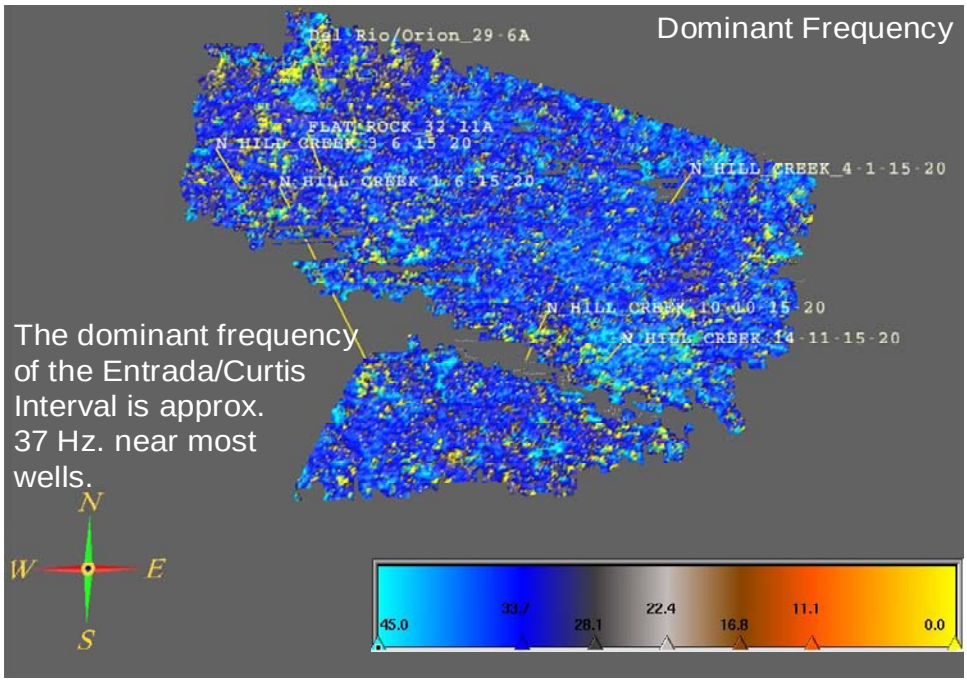


Figure 21: Dominant frequency map for a 28 ms window around the Entrada/Curtis Interval. Notice most of the map is one color. Most of the Entrada/Curtis interval has a dominant frequency near 37 Hz.

**Average Instantaneous Phase.**

Average instantaneous phase appears to have limited value in interpreting the Entrada/Curtis-Moab interval given the other attributes available to the interpreter. Dune complexes appear to have consistent phase values. Other features which are less easily interpreted include lineaments in the east central portion of the northern structural block and a dark sinuous feature visible in the northwest potion of the survey (Fig. 22). These lineaments are likely an acquisition footprint and do not represent anything of geological significance. It is possible that the dark sinuous feature may represent a major muddy channel as part of a wadi system during Entrada/Curtis time.

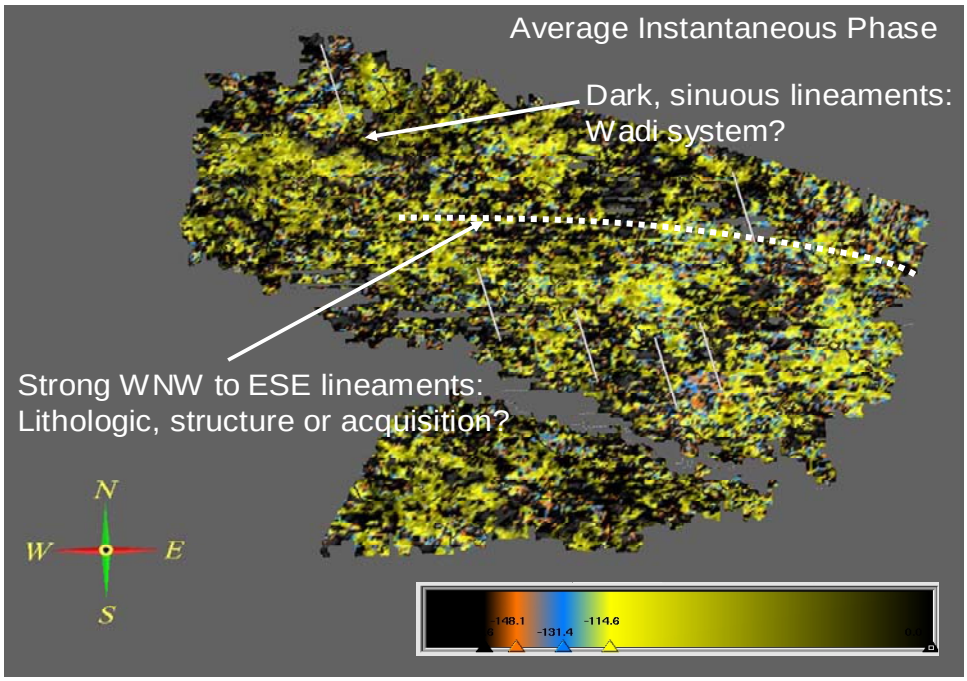


Figure 22: Average instantaneous phase attribute map. Areas where dune complex geometry has been previously noted appear to have fairly consistent phase values. Max peak amplitude appears to provide better constraints and resolution on dune complex geometry thus average instantaneous phase has limited value in interpretation.

**Semblance (ESP)**

The semblance extraction map assists the interpreter in defining the edges of dune complexes (Fig. 23). Black areas are interpreted to represent interdune facies whereas light blue colors represent the dune complexes. A blue circular geometry can be observed surrounding the well located in the northwest portion of the survey (DelRio/Orion 29-6A). This circular geometry outlines one of the thickest Entrada/Curtis sections within the survey. Again, this thickened section may be related to a lack of Entrada erosion or an anomalously thick Curtis section (Fig. 15). The DelRio/Orion 29-6A well has drilled this anomaly and is one of the most prolific gas producers in the NHC area.

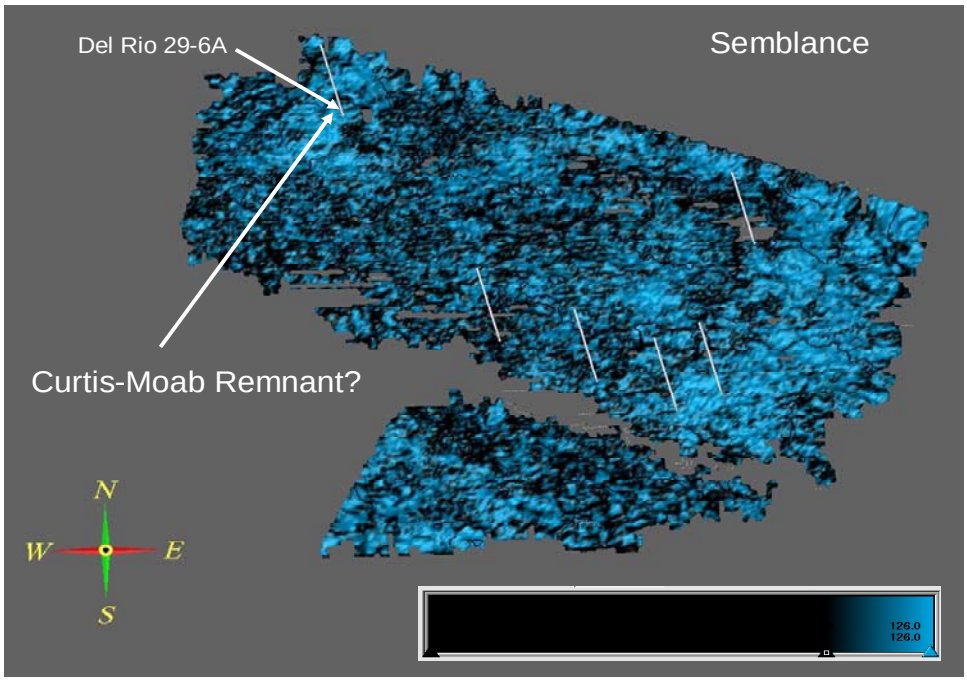


Figure 23: Semblance map extracted from a 24 ms window around the Entrada/Curtis interval. Semblance values were taken from 10 ms below the Entrada/Curtis pick. Blue color represents similar zones and black color represents similar zones. Black likely represents the edges of dune complexes while blues represent the aerial extent of dune complexes.

**Spectral Decomposition**

Spectral decomposition appears to be useful in delineating lateral changes in the thickness of dune complexes. As we slice through different frequencies of our calculated frequency volume, theoretically we should be able to image portions of the dune complexes with varying sand thickness. As we move from lower frequencies to higher frequencies, we would expect to image progressively thinner portions of the dune complexes. This becomes apparent as we focus on the dashed circle within Figures 24, 25 and 26. As we extract a 20 Hz frequency slice from the frequency volume, we don't see much in the way of tuning within our zone of interest

(Fig. 24). As we increase the frequency to 35 Hz we begin to see the thinner portions of the dune complex beginning to tune (Fig. 25). If we increase the frequency to 50 Hz we again tune the even thinner portions of the dune complex (Fig. 26). Based on this exercise, we are then able to qualitatively view lateral changes in dune thickness. In this case the dune complex appears to be thickest just south of well 14-11 (within dashed circle) and thins to the north.

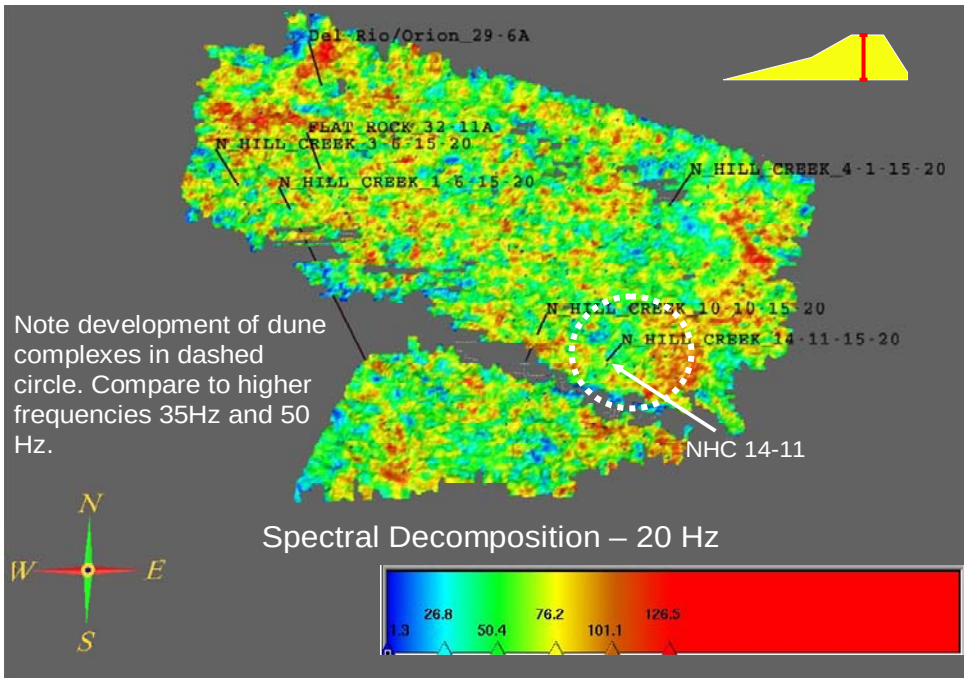


Figure 24: Spectral Decomposition 20 Hz tuning map extracted from a 40ms window around the Entrada/Curtis interval. Reds represent highest amplitudes due to tuning at 20 Hz. Notice the lack of tuning in the portion of the dune complexe represented by the dashed circle. Also notice the schematic diagram in the upper right which represents the part of the dune we are imaging with a particular frequency. Compare with spectral decomposition maps at 35 Hz and 50 Hz. (Modified after Keach et. al., 2006)

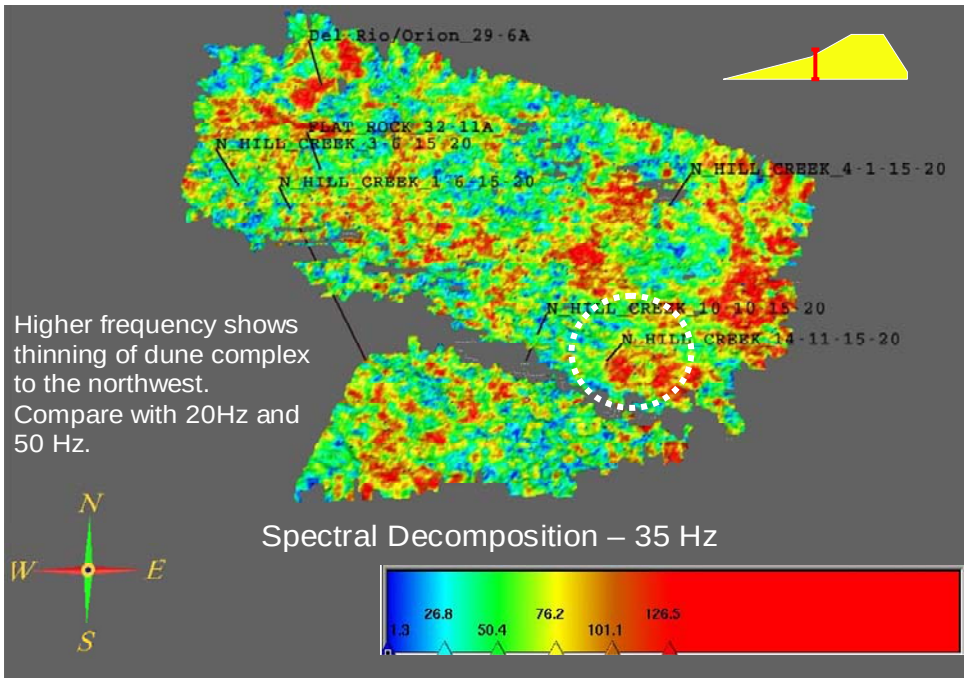


Figure 25: Spectral Decomposition 35 Hz tuning map extracted from a 40ms window around the Entrada/Curtis interval. Reds represent highest amplitudes due to tuning at 35 Hz. Notice that portions of the dune complexe in the circle are beginning to tune. Notice also the schematic diagram in the upper right which represents the part of the dune complex we are imaging with a particular frequency. Compare with spectral decomposition maps at 20 Hz and 50 Hz (Modified after Keach et. al., 2006)

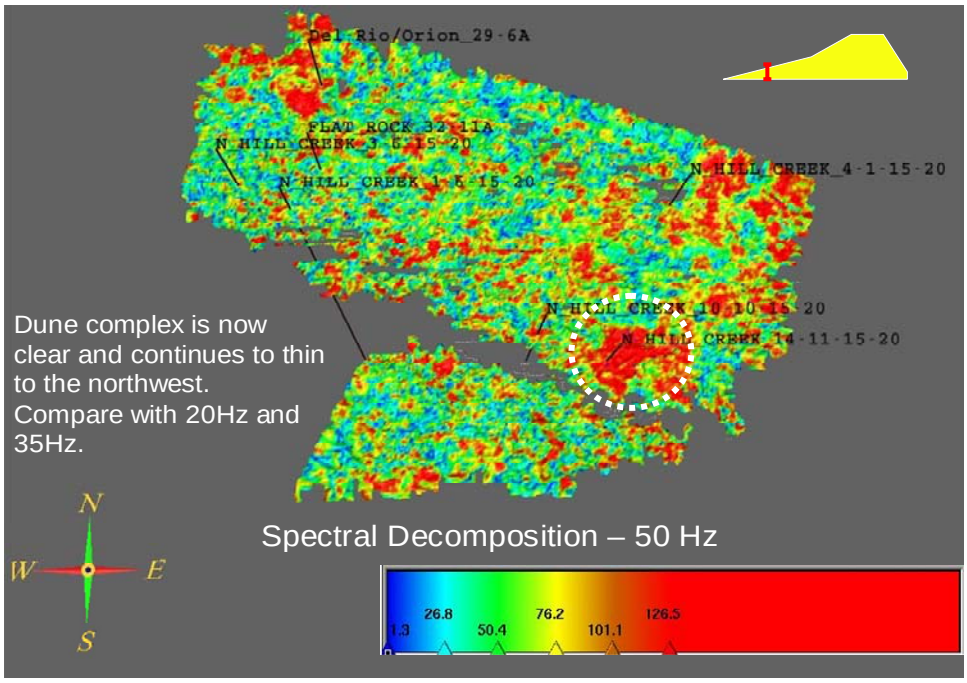


Figure 26: Spectral Decomposition 50 Hz tuning map extracted from a 40ms window around the Entrada/Curtis interval. Reds represent highest amplitudes due to tuning at 50 Hz. Notice portions of the dune complex are beginning to tune in the left circle. Notice also the schematic diagram in the upper right which represents the part of the dune complex we are imaging with a particular frequency. Compare with spectral decomposition maps at 20 Hz and 35 Hz (Modified after Keach et. al., 2006)

**Entrada/Curtis Isochron Map**

The Entrada/Curtis isochron map shows time thickness anomalies mostly in the western portion of the NHC seismic survey (Fig. 27). Most of the wells that have been drilled appear to be positioned on Entrada/Curtis thickness anomalies. These wells, however, range greatly in production. The best wells appear to be associated with thick Entrada/Curtis intervals in association with structural or stratigraphic relief. These thick Entrada/Curtis areas may be associated with preserved Entrada/Curtis dune relief like that

near Del Rio/Orion 29-6A, but more likely are a result of shortening and deformation due to compressional stress.

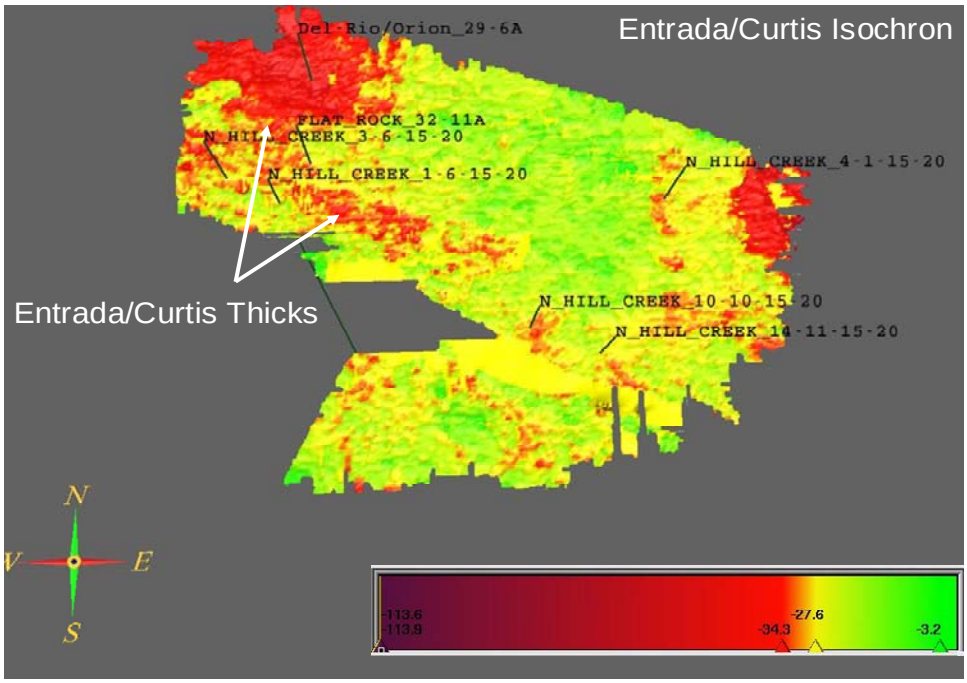


Figure 27: Entrada/Curtis Isochron map. Reds represent Entrada/Curtis time thickness anomalies while greens and yellows represent intervals near 25 ms in thickness. Notice that most wells aim to exploit these thickness anomalies.

## Well-to-Seismic Correlation

### Introduction

Quantification of well and seismic attributes by means of cross plotting may be useful to the explorationist. Detection of trends between these data can lead to a better understanding of reservoir character and provide a foundation for better reservoir management. These trends may also allow interpreters in surrounding areas to infer physical rock properties based on the seismic response when well control is limited.

There are many steps that precede cross plotting, most of which involve some form of quality control. Well log editing for the purpose of well to seismic correlation, when done properly, can often lead to excellent synthetic seismograms and well to seismic correlation (Box et. al., 2004). It is essential that well logs receive editing to limit the number of bad data points. It is also important to correlate the well logs to the seismic data which by doing so, the interpreter can constrain his or her zone of interest. This type of correlation provides ground truth to the interpreted seismic data which otherwise is largely based on interpretation and ensures that the cross plotted values coincide.

The Entrada/Curtis interval is the primary zone of interest although the Dakota Silt (DS) has proven to be useful in well-to-seismic correlation. The DS is easily picked on well log and seismic data. By hanging generated synthetics on the DS, the Entrada/Curtis was easily correlated.

**Well Log Editing**

Key logs from wells that contain the Entrada/Curtis interval were the only logs edited within the NHC seismic survey. Quality control methods were applied to the logs to pick out areas affected by borehole rugosity which appeared to be the most common cause of bad data. Sonic and density logs within six key wells were edited for the purpose of synthetic seismogram generation and well-to-seismic correlation. These six wells lie inside the North Hill Creek (NHC) survey and have all penetrated the Entrada/Curtis interval. There are, however, eleven Entrada/Curtis penetrating wells used in the cross plotting of well and seismic attributes. There are 15 total wells that penetrate the Entrada/Curtis, but data was limited to the eleven considered in this study.

Sonic and density logs were compared with caliper and gamma ray logs in order to flag zones affected by borehole rugosity (Fig. 28).

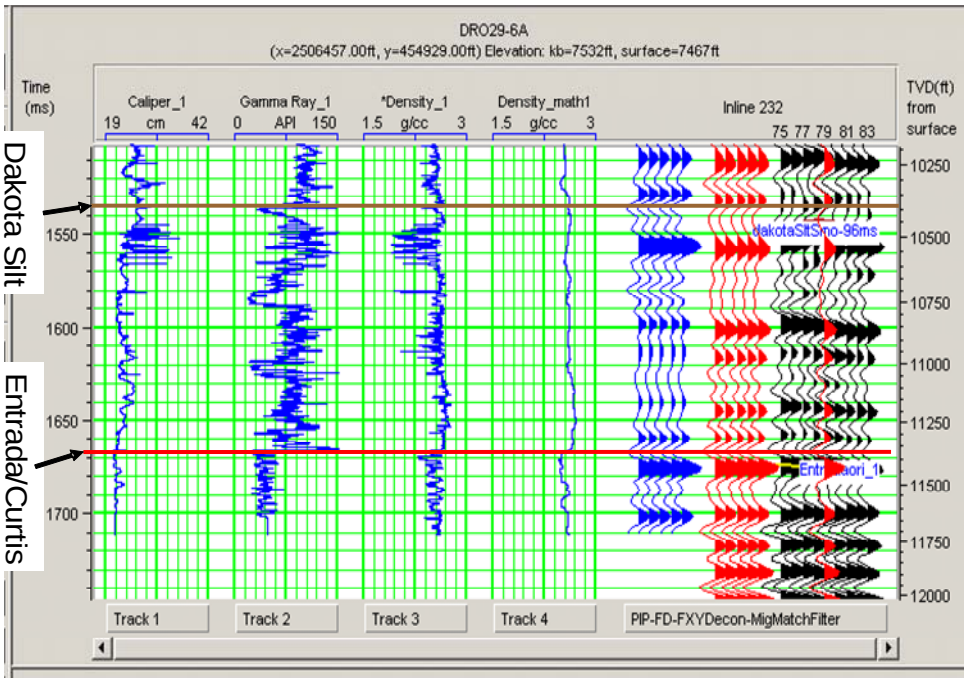


Figure 28: DelRio/Orion 29-6A. Example of well log editing display that we found to be useful. Track 1: caliper log. Track 2: gamma ray log. Track 3: original density log. Track 4: edited density log. Original seismic data (black) shown with Dakota silt and Entrada/Curtis picks. Synthetic seismogram (blue) generated with edited density and sonic logs. Composite seismic trace (red) calculated from real seismic traces around the borehole.

Areas with bad data directly related to borehole rugosity such as large changes in velocity and density were flagged. A median filter was placed on all logs to limit abundant small spikes in the data. The median filter operation replaces the sample value at the center of the operator with the median of the sample values contained within the operator. The larger the operator length, the smoother the log. This process was largely experimental in order to isolate the best log operator length which is 100. If the operator length was too small, spikes in the data might be preserved, therefore affecting future cross plots and

synthetic interpretation. Conversely, if the operator was too large (i.e. too much smoothing) the crossplots might not be representative of the data and synthetics would not provide adequate detail for seismic correlation. Larger zones affected by borehole rugosity that were not corrected by the median filter were then hand edited.

**Wavelet Extraction**

A wavelet was extracted using edited input data from NHC well 10-10 and a 60ms wavelength, constant phase, 25ms taper length wavelet. Normally a statistical wavelet would be extracted from the seismic data in order to correlate the well and seismic data. Use of this statistically extracted wavelet provides a general correlation, but mathematically a higher correlation value can be achieved. In order to get the best correlation, the statistical wavelet extraction would be followed by a well-based wavelet extraction. This process was not used in this study because our primary focus was to give our Entrada/Curtis poststack seismic interpretation ground truth, not to achieve the best correlation between a full trace and all the well log data. We also compared synthetics generated by convolving extracted wavelets from an edited log suite and a non-edited log suite with their associated reflection series. We found that using the extracted wavelet from the edited log suite created a better well-to-seismic tie than the non-edited log based wavelet (Fig. 29). The difference in the mathematical correlation between the edited and non-edited based synthetic seismogram was approximately 0.10 or 10%.

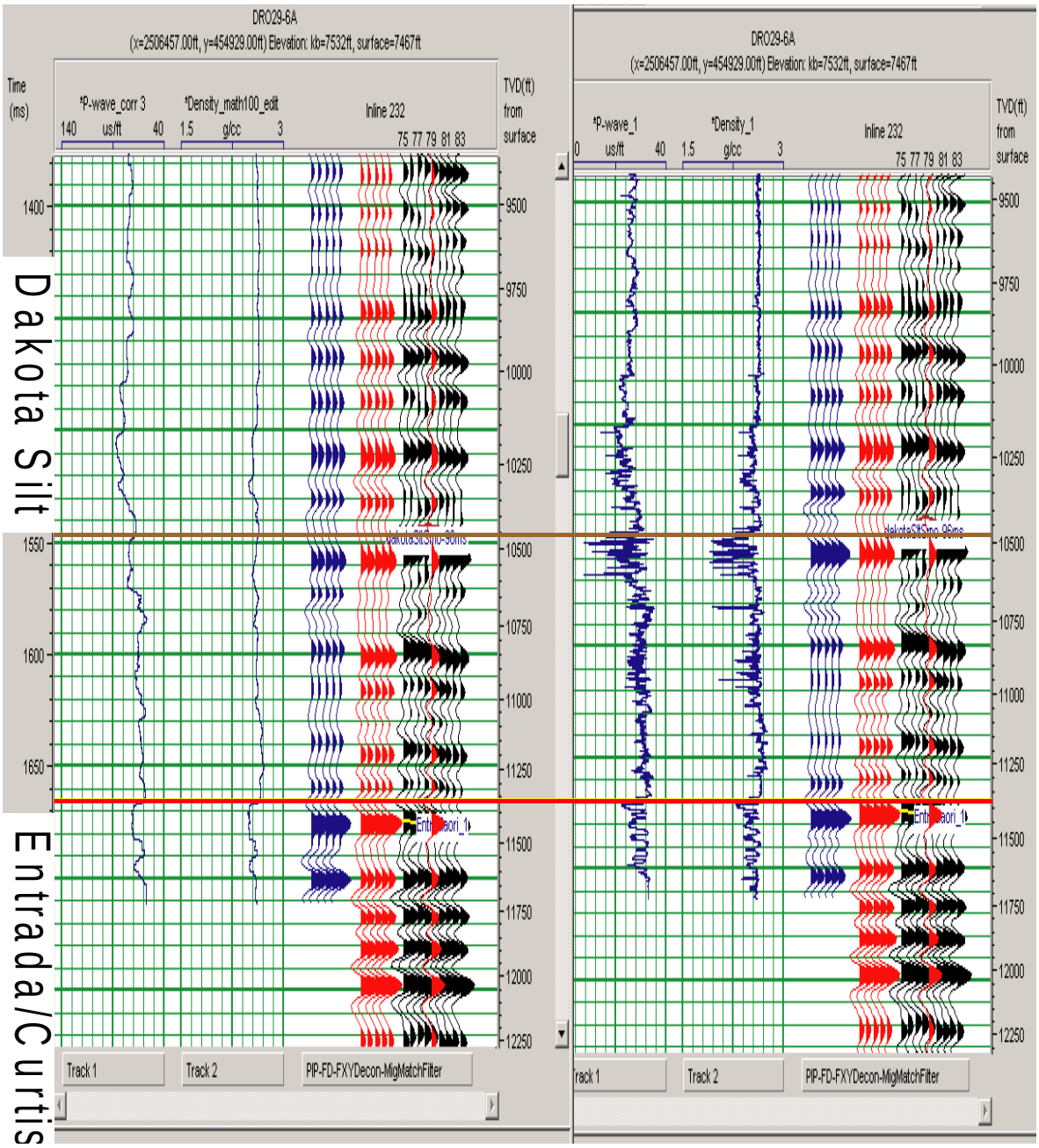


Figure 29: Example of synthetic traces generated from convolving an extracted wavelet with the reflection series from edited and non-edited logs from the DelRio/Orion 29-6Awell. The synthetic traces are in blue, the seismic composite trace is in red and the poststack seismic is in black. Dakota Silt and the Entrada/Curtis horizons are shown as well. Left: edited version. Right: non-edited version.

**Synthetic Seismogram Generation**

After quality controlling the data, synthetic seismograms were generated. Many different synthetics were generated using input logs with different median filter operator lengths. We found that an operator length of 100 provided adequate smoothing. Synthetics were compared to composite traces that are generated by taking an average of a given number of traces around the borehole. As a result of convolving the edited well log reflection series with the extracted wavelet from the NHC well 10-10, and placing a -55º phase shift on the synthetic, we were able to generate a very good well-to-seismic tie in our zone of interest (Fig. 14). As mentioned earlier however, the Entrada/Curtis interval is defined by the seismic trough above our previously interpreted peak. This shows the importance of generating synthetic seismograms for the purpose of well-to-seismic correlation. This has caused us to choose an analysis window for seismic attribute extraction that includes this seismic trough.

**Editing and Well-to-Seismic Correlation Workflow:**

I. Load LAS or ASCII files into HR database.

II. Load the correlative 3D volume into HR for log to seismic correlation.

III. QC log data and pick out areas that may have bad data due to borehole rugosity. Display gamma ray, caliper, density, sonic and any other logs that might be useful to the editor.

IV. Edit logs by means of filtering and hand-editing.

V. Extract a wavelet using input well data. Experiment with different input wavelengths to find the most representative wavelet.

VI. Generate synthetics using a combination of extracted wavelets and edited well logs. Pick the filter length and extracted wavelet that appear to generate the best ties (the use of multiple extracted wavelets might be necessary).

## Seismic and Well Log Attribute Quantification - A Summary

Seismic and well log values used for quantification were taken from the Entrada/Curtis interval. Numerous petrophysical values from well logs were cross plotted with extracted seismic attributes values. Most of the log values are average values over the entire Entrada/Curtis interval. Only the plots with significant relationships are discussed here. Regression lines with $R^2$ values are shown on cross plots (Fig. 30; Figs. 33-39) and give statistical support to our interpretation.

As we cross plotted the data, it became apparent that NHC wells 1-9 and 4-1 were outliers. The following interpretations are largely based on the relationship between physical rock properties and amplitude anomalies. Wells 1-9 and 4-1 are located in areas where amplitude statistics are anomalously low. Therefore, regression lines and $R^2$ values have been computed with and without these outlying values (Table 2).

| Cross plot | Regression | $R^2$ | Best Regression w/outliers | $R^2$ | Best Regression w/out outliers | $R^2$ |
|---|---|---|---|---|---|---|
| Thickness vs. Cumulative Production | linear | 0.5886 | logarithmic | 0.6882 | logarithmic | 0.7809 |
| Avg. Reflection Strength vs. Avg. Porosity | linear | 0.2298 | 5th order polynomial | 0.4358 | 5th order polynomial | 0.7316 |
| Max. Peak Amplitude vs. Avg. Porosity | linear | 0.0345 | 3rd order polynomial | 0.0439 | 3rd order polynomial | 0.6555 |
| Energy Half-Time vs. Avg. Porosity | linear | 0.0713 | 3rd order polynomial | 0.4318 | 3rd order polynomial | 0.3901 |
| Dominant Frequency vs. Avg. Porosity | | dominant frequency remains constant as porosity increases | | | | |
| Max. Peak Amplitude vs. Gamma Ray | linear | 0.4165 | exponential | 0.4492 | exponential | 0.2624 |

Table 2: Cross plot data with associated regression and $R^2$ data. An $R^2$ value has been computed for a linear regression, a best regression w/ outliers and a best regression w/out outliers for each cross plot. The best regression type differs for each data set. Notice the $R^2$ values from average reflection strength and maximum peak amplitude cross plots increase dramatically when outliers are removed.

We have found that the best producing wells in the NHC survey area are associated with the thickest Entrada/Curtis sections and are positioned in locations that exploit structural or stratigraphic highs (Fig. 30; Fig. 31). Maximum peak amplitude also appears to correlate with production, but seems to be secondary to structure (Fig. 32). Some amplitude highs within the survey have been drilled and are very productive, however, these amplitudes are usually associated with structural or stratigraphic relief. Wells drilled on amplitude highs that are not associated with significant structural or stratigraphic relief are among the lowest gas producers within the NHC survey area.

In general, the average reflection strength (Fig. 33; Fig. 34), maximum peak amplitude (Fig. 35; Fig. 36) and energy half-time (Fig. 37) increase as average porosity increases. Average porosity however, seems to be less important than the thickness of

the Entrada and its position relative to structural or stratigraphic relief. Zones of higher porosity do not relate to zones of highest gas production. In fact, the two most productive wells in the NHC survey have been drilled in areas where average porosity is near 4%. However, these productive areas as well as lower producing areas, have zones of maximum porosity between 14% and 20%. These high porosity zones can often be up to 40 ft (12 m) thick.

The dominant frequency of the Entrada/Curtis interval appears to range from 30 to 40 Hz (Fig. 38).

One apparent relationship exists between gamma ray (API) number and max peak amplitude (Fig. 39). Most average gamma ray values for the Entrada/Curtis interval are generally confined to a range of 40 API to 58 API. These low API values are also generally associated with high amplitudes. There are a few exceptions. The highest API values are found in NHC wells 1-9 and Flat Rock 32-11A which are associated with lower amplitudes. NHC well 4-1 appears to have similar API values as the other wells but is anomalous in that it is associated with a lower amplitude. This well is not associated with any structural or stratigraphic relief. These three wells are among the lowest producers in the NHC area. In general, amplitude highs relate to the "cleanest" (i.e. low shale) Entrada/Curtis zones within the NHC survey.

Spectral frequency values were cross plotted with Entrada/Curtis thickness and net sand values. We hoped that we would see a relationship between these data as it would have provided ground truth to our spectral decomposition interpretation. This was not the case. Upon cross plotting the data, we found essentially no relationship. This

may be due to the window length chosen in our spectral decomposition analysis and the fact that net sand values were over the entire Entrada/Curtis interval. Numerous zones of alternating sandstone and siltstone are common throughout the Entrada/Curtis interval. This causes tuning at different frequencies due to different sandstone thicknesses in the same location. Therefore, it is not possible to isolate a specific sand thickness for a specific tuning event at a given frequency. One way to find the relationship between sand thickness and spectral frequency may be to decrease the window length and analyze sand bodies of a known thickness. This becomes problematic, however, as the error in calculating spectral decomposition increases greatly when the window length is below 20 samples (Keach, 2007; personal communication). The window length we have chosen for spectral decomposition analysis is 20 samples. The nature of the Entrada/Curtis interval does not appear to be prime for quantitative spectral decomposition analysis but spectral decomposition is useful in a qualitative sense.

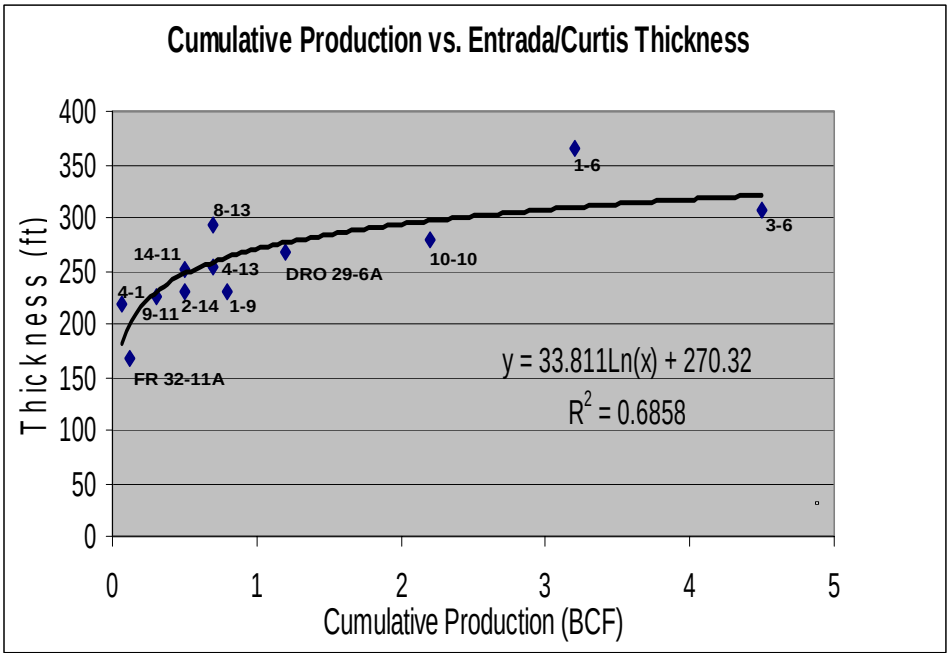


Figure 30: Cumulative Production is the greatest in areas where the Entrada/Curtis interval is thickest. The best producing wells also appear to be associated with structural highs (Fig. 32) and high amplitudes (Fig. 33).

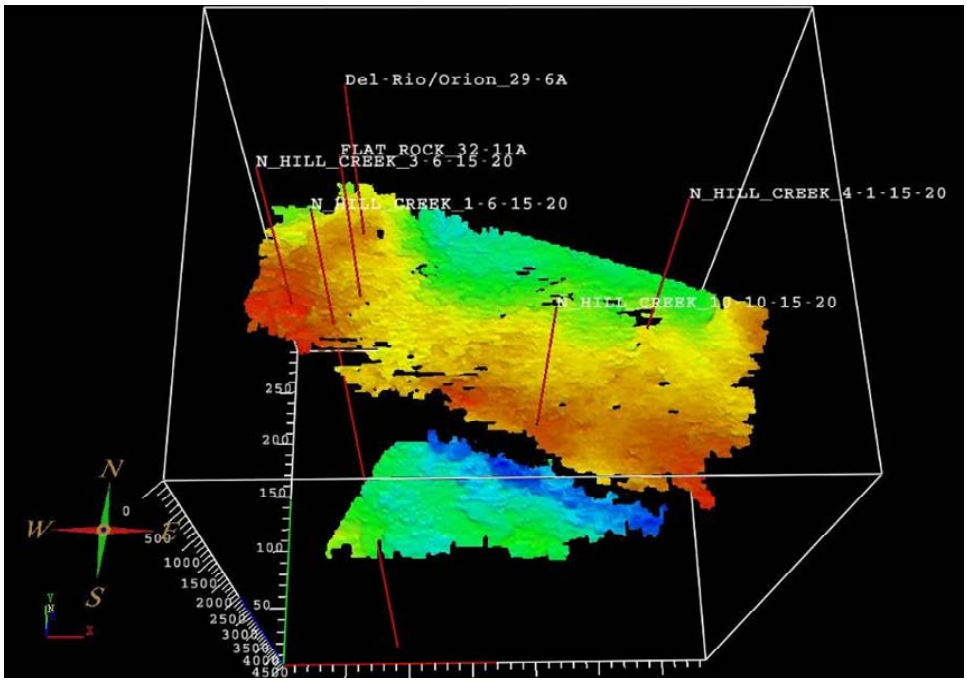

Figure 31: Time structure map of the interpreted Entrada/Curtis horizon. The warmer colors represent structural highs while the cooler colors represent structural lows. The DelRio/Orion 29-6A and NHC wells 3-6, 1-6 and 10-10 are the best gas producers in the NHC survey area and are associated with structural or stratigraphic highs. The Flat Rock and NHC 4-1 have produced significantly less and are not associated with structure.

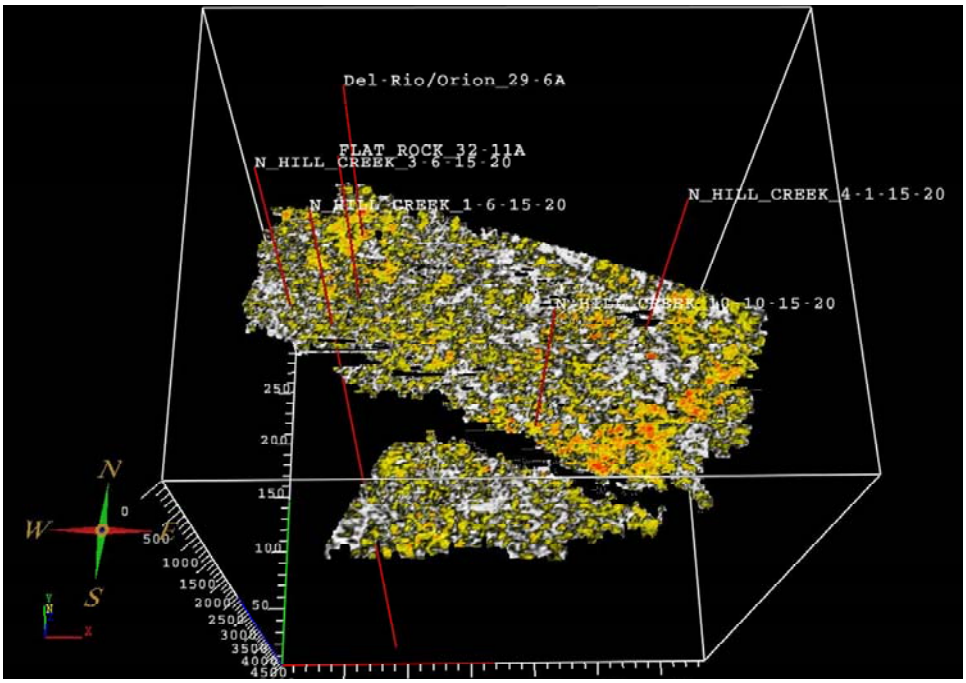

Figure 32: Max peak amplitude extraction with a window length of 28 ms (6 ms above, 22 ms below). Notice that the best wells generally are associated with maximum peak amplitude anomalies but some of the anomalies aren't very laterally extensive whereas all of the best wells are associated with structural or stratigraphic relief (Fig. 32).

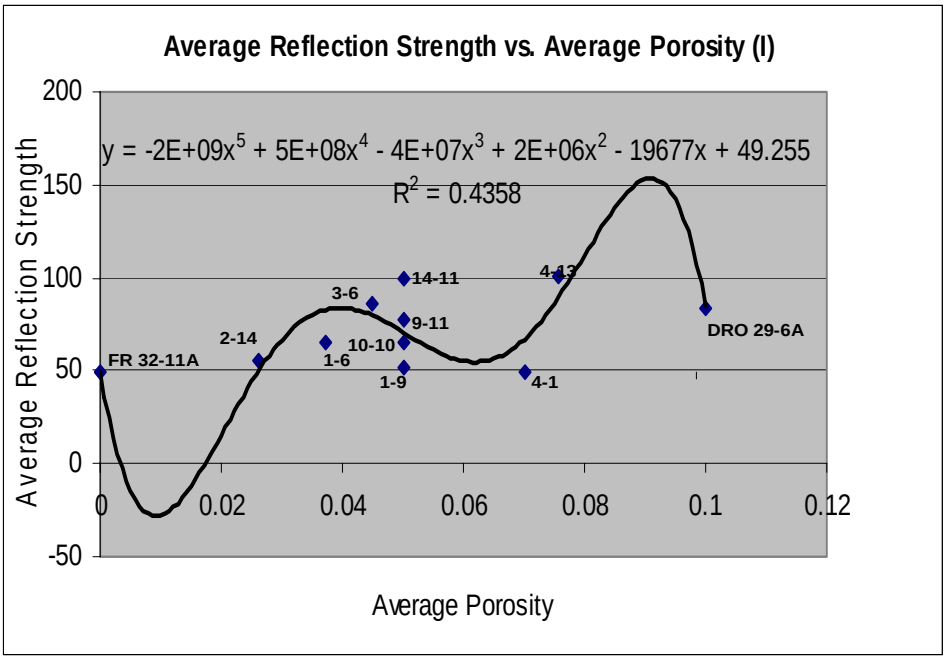


Figure 33: In general, zones of higher average porosity correspond to greater average reflection strength and greater peak amplitude. Notice the $R^2$ value before and after (Fig. 35) outlier values from wells 1-9 and 4-1 are removed.

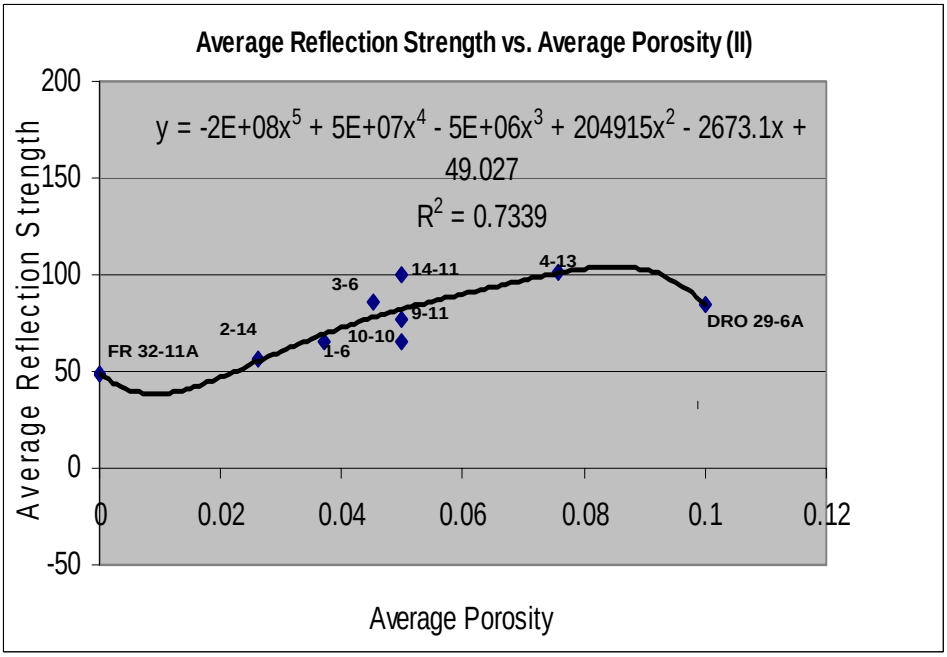


Figure 34: In general, zones of higher average porosity correspond to greater average reflection strength and greater peak amplitude. Notice the higher $R^2$ when outliers from wells 1-9 and 4-1 are removed.

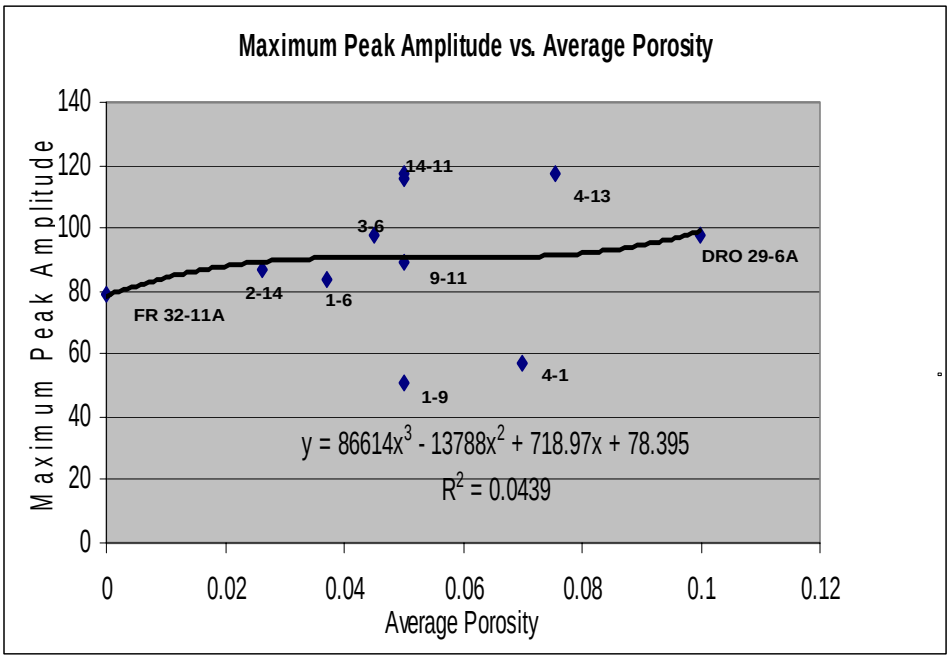


Figure 35: In general, zones of highest average porosity are related to zones of highest amplitudes. Notice the extremely low $R^2$ value. This is due to the two outliers (wells 1-9 and 4-1). When these outliers are removed and a 3rd order polynomial is derived, the $R^2$ value increases dramatically (Fig. 37).

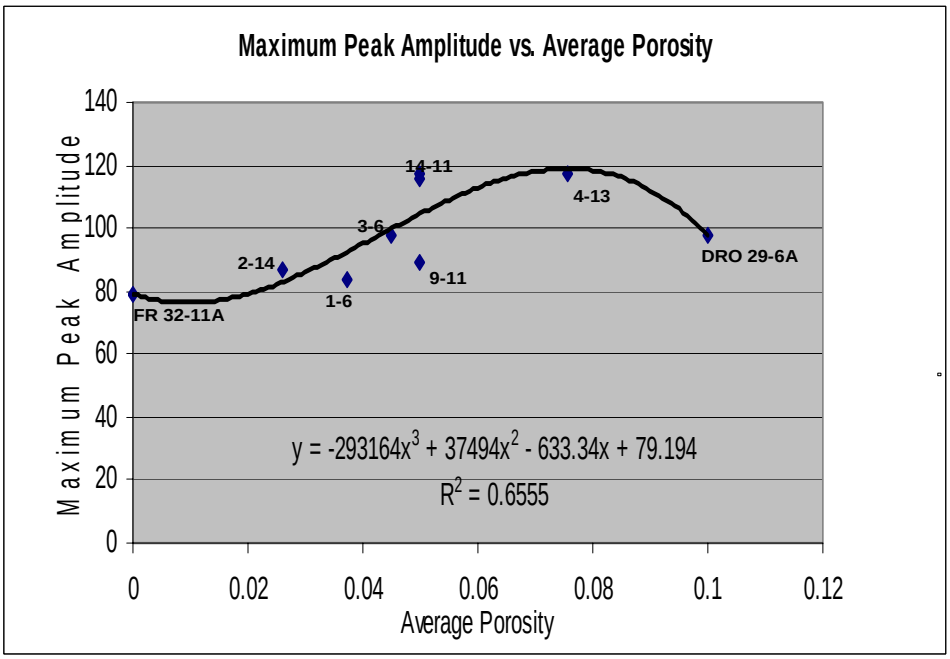


Figure 36: Notice the dramatic increase of the $R^2$ value when the two outliers from Figure 35 are removed. In general, maximum peak amplitude increases as porosity increases.

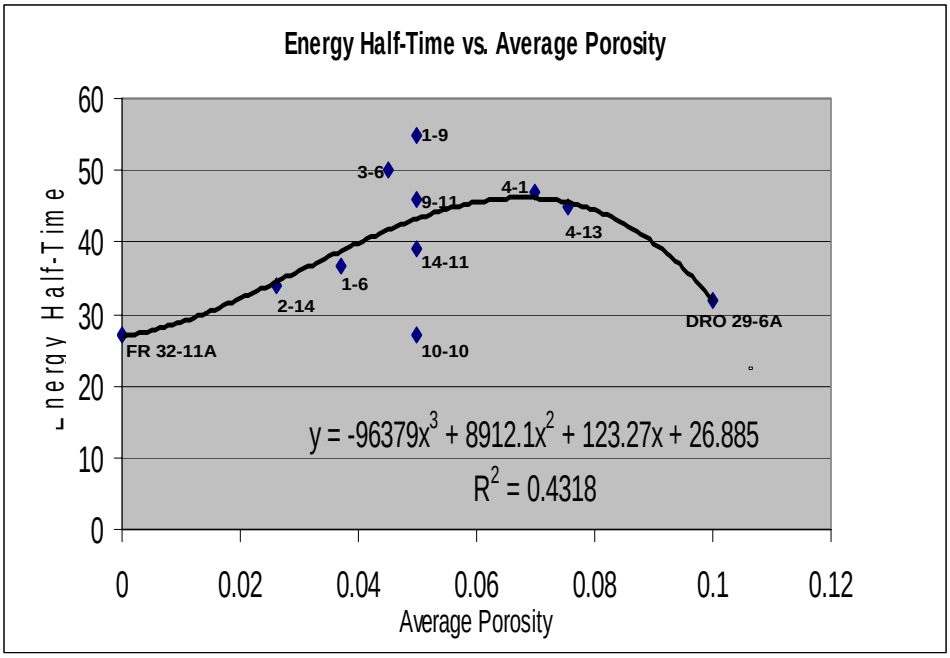


Figure 37: In general, energy half-time increases as average porosity increases except near wells 10-10 and Del Rio/Orion 29-6A.

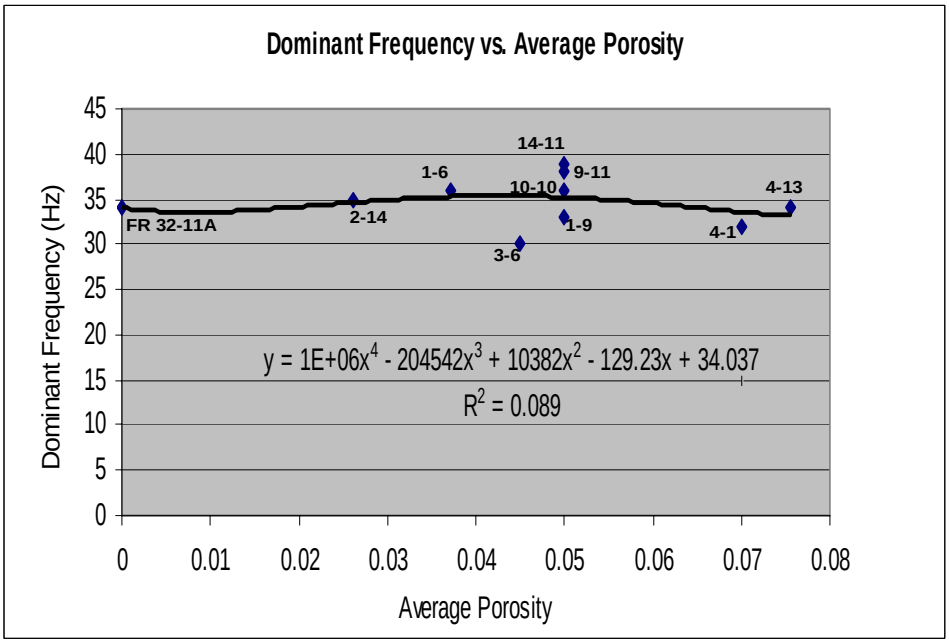


Figure 38: The dominant frequency of the Entrada interval in approximately 36 Hz and is independent of average porosity.

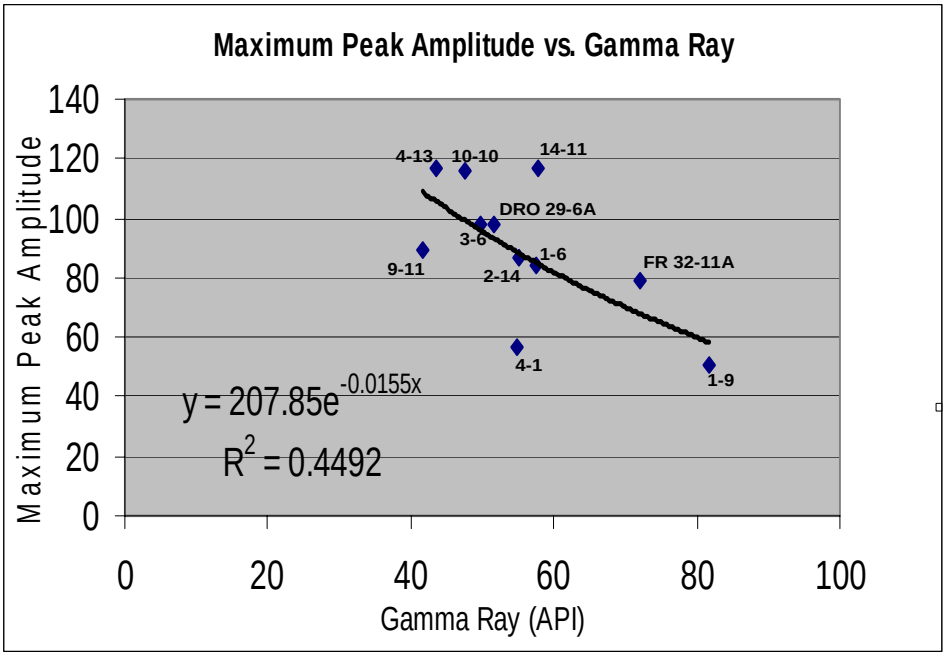


Figure 39: In general, the higher the amplitude, the lower the gamma ray value. Assuming lower gamma ray values represent cleaner sandstones, then zones of high amplitude represent sandstone lithologies with the least clay.

## Conclusions

Qualitative and quantitative seismic and well log attribute analysis within the Entrada/Curtis interval of the North Hill Creek 3D seismic survey has proven to be useful in describing reservoir geometry and relating seismic data to physical rock properties. This may aid future explorationists focusing on the Entrada/Curtis interval in high-grading prospects and more efficiently exploiting this play.

We have observed that the best producing zones within the NHC survey are associated with the thickest Entrada/Curtis sections (>260 ft., 79 m) and are located where structural highs or stratigraphic traps are present. The thickest Entrada/Curtis

intervals can be found by creating an isochron map. Generating this map however is problematic since the underlying Carmel Formation lacks a laterally continuous seismic reflector. The best structural and stratigraphic traps or those with the greatest relief are found in the western portion of the survey. The Entrada/Curtis play in the NHC survey area appears to be primarily a structural play with the exception of the stratigraphic trap in which the DelRio/Orion 29-6A is located . This, however, does not discount the need for the presence of an adequate reservoir.

We have also observed that the zones of best production are associated with low gamma ray (low API) values. These low values appear to be directly related to zones of high amplitude. Thus, maximum peak amplitude as a seismic attribute delineates areas of higher sand content (i.e. dune complexes) whereas zones of low amplitude represent areas of lower sand content (i.e. muddier interdune or tidal flat facies). The areas of highest sand content or the highest laterally extensive max peak amplitude anomalies are located in the eastern portion of the survey. Porosity generally correlates to max peak amplitude in that as it increases, so does the amplitude. This peak may also be accentuated due to the presence of gas. Lack of significant average porosity, however, does not seem to be related to a lack of production. In fact, the best producing wells have been drilled in Entrada/Curtis intervals where average porosity is near 4 %. These low average porosity zones, however, have isolated zones of much higher porosity, usually in the upper portion of the Entrada/Curtis interval, and are in areas where structural relief is present. These higher porosity zones can be seen in outcrop east of Grand Junction, Colorado (Fig. 7).

Spectral decomposition may be useful in delineating lateral changes in dune complex thickness. In the NHC survey area, where dune complexes are interpreted to be present, spectral decomposition as a seismic attribute has shown these complexes to be thickest to the south and thinnest to the north. Quantitative relationships between spectral frequency and net sand do not seem to exist based on the window length we have chosen.

Semblance generally is useful in delineating lateral facies changes but appears to be secondary to max peak amplitude and average reflection strength. Average instantaneous phase is of little value compared to the other attributes we have extracted.

Splits in the Entrada/Curtis seismic reflector should be sought after as this may represent preserved Entrada dune relief or an additional thick Curtis section. The drilling of this anomaly in the NHC survey area has led to a very productive well.

The above conclusions are supported by regression lines and $R^2$ values. Each generated cross plot displays an association between well and seismic data that is not necessarily linear. These relationships are often better represented by a regression line in the form of a polynomial, logarithm or exponential equation. When outlying values from NHC wells 1-9 and 4-1 are removed, the $R^2$ values improve greatly for maximum peak amplitude and average reflection strength.

References

Cited:

Bahorich, M., and Farmer, S., 1995, 3-D seismic discontinuity for faults and stratigraphic features: The coherence cube: The Leading Edge, v. 14, p. 1053.

Barbeau, D.L., 2003, A flexural model for the Paradox Basin; implications for the tectonics of the ancestral Rocky Mountains: Basin Research, v. 15, p. 97.

Blakey, R.C., 1988. Basin tectonics and erg response. Sedimentary Geology, v. 56, p 127-151.

Box, R., Maxwell, L., Loren D., 2004. Excellent synthetic seismograms through the use of edited logs: Lake Borgne Area, Louisiana, U.S. The Leading Edge, v. 23, p. 218-223.

Chan, M.A., 1989, Erg margin of the Permian White Rim Sandstone, SE Utah: Sedimentology, v. 36, p. 235-251.

Currie, B.S., Reeder, M.D., 2002, Sequence Stratigraphy of the Jurassic Curtis, Summerville and Stump Formations, Utah-Colorado: Geological Society of America 2002 Denver Annual Meeting, Stratigraphy (Posters) II., Session No. 124—Booth #109

Eckels, M.T., Suek, D.H., and Harrison, P.J., 2005, New, old plays in southern Uinta basin get fresh look with 3D seismic technology: Oil & Gas Journal, v. 103, p. 32-40.

Eckels, M., Suek, D., Rawn-Schatzinger, V., Weyland, V., and Harrison, P., 2006, Applying 3D Seismic to Underexplored Areas in the Uinta Basin: Search and Discovery Article # 10097

Fryberger, S.G., Al-Sari, A.M., and Clisham, T.J., 1983, Eolian dune, interdune, sand sheet, and siliciclastic sabkha sediments of an offshore prograding sand sea Dhahran area, Saudi Arabia: AAPG Bulletin, v. 67, p. 280-312.

Fryberger, S.G., 1986, Stratigraphic traps for petroleum wind-laid rocks: AAPG Bulletin, v. 70, p. 1765-1776.

Hintze, L.F., 1988, Geologic History of Utah, Brigham Young University Geology Studies, Special Publication 7, 202 p.

Heideman, M.T., Johnson, D.H., Burrus, S.C., Gauss and the history of the fast Fourier transform: Archive for History of Exact Sciences, v. 34, 1985

Imlay, R.W., 1980, Jurassic paleobiogeography of the conterminous United States and its continental setting: U.S. Geological Survey Professional Paper 1062, 134p.

Keach, R.W. II, Morris, T.H., McBride, J.H., Mullen, M., Leetaru, H.E., and O'Neal, R., Interpretation of the Jurassic Entrada Sandstone play using 3D seismic attribute analysis, Uinta Basin, Utah, Utah Geological Survey, Open File Report-493, CD.

Kocurek, G., 1981, Erg reconstruction; the Entrada Sandstone (Jurassic) of northern Utah and Colorado: Palaeogeography, Palaeoclimatology, Palaeoecology, v. 36, p. 125.

Kocurek, G., 2000, Catastrophic flooding of an Aeolian dune field: Jurassic Entrada and Todilto Formations, Ghost Ranch, New Mexico, USA: Sedimentology, v. 47, p. 1069

Marino, J.E. and Morris, T.H., 1996, Erg Margin and Marginal Marine Facies Analysis of the Entrada Sandstone, Utah: Implications to Depositional Models and Hydrocarbon Entrapment, in Morales, M., ed., Continental Jurassic Symposium Volume, Museum of Northern Arizona, Flagstaff, Arizona, p. 483-496.

Mitchum, R.M., Jr., Vail, P.R., and Thompson, III, S., 1977. Seismic stratigraphy and global changes in sea level, part 2: The depositional sequence as a basic unit for stratigraphic analysis. In: Payton, C.E. ed., Seismic Stratigraphy—Application to Hydrocarbon Exploration. AAPG Mem. 26, 53-62, 1977.

Monn, W.D., 2006, A multidisciplinary approach to reservoir characterization of the coastal Entrada erg-margin gas play, Utah, Brigham Young University, MS thesis, 33 p.

Morris, T.H., McBride, J.H., and Monn, W.D., 2005, A Multidisciplinary Approach to Reservoir Characterization of the Coastal Entrada Erg-Margin Gas Play, Utah, Utah Geological Survey, Open File Report 459, CD.

Partyka, G.A., Gridley, J.M., and Lopez, J., 1999, Interpretational Applications of Spectral Decomposition in Reservoir Characterization, The Leading Edge, v. 18, pg 353-360

Potter, S., and Hayden, A., 2006, Paleoenvironmental Interpretation of the "Board Beds" Unit of the Entrada Formation, Western Colorado, USA.: Abstract : Rocky Mountain Section-58th Annual Meeting, Session No. 4—Booth# 9.

Rigby, K.J., 1978, Jurassic plant fossils from the Walloon Coal Measures at Rosewood Consolidated Colliery: Queensland Government Mining Journal, v. 79, p. 526-529.

Stokes, W.L., 1988, Geology of Utah, 2nd ed., Utah Geological and Mineral Survey.

Taner, M.T., and Sheriff, R.E., 1977, Application of amplitude, frequency, and other attributes to stratigraphic and hydrocarbon determination, In: Payton, C.E. ed., Seismic Stratigraphy-Application to Hydrocarbon Exploration. AAPG Mem. 26, 301-327.

Vincelette, R.R. and Chittum, W.E., 1981, Exploration for oil accumulations in Entrada Sandstone, San Juan Basin, New Mexico: AAPG Bulletin, v. 65, p. 2546-2570.

White, R.E., 1991 Properties of instantaneous seismic attributes: Geophysics: The Leading Edge of Exploration, v. 10, p. 26.

Not Cited:

Anderson, O.J., 2000, Jurassic stratigraphy at Placitas, New Mexico and its regional significance: Abstracts with Programs - Geological Society of America, v. 32, p. 458.

Benan, A.A., 2000, Catastrophic flooding of an aeolian dune field; Jurassic Entrada and Todilto formations, Ghost Range, New Mexico, USA: Sedimentology, v. 47, p. 1069.

Bracewell, R. N., 1965, The Fourier transform and its applications: McGraw-Hill Book Co.

Brown, Alistair R., Interpretation of Three-Dimensional Seismic Data, Fifth ed., AAPG Memoir 42, SEG Investigations in Geophysics, No. 9, Tulsa, Oklahoma: 1999 AAPG,SEG

Case, J.E., 1992, Map showing interpretation of geophysical anomalies of the northwestern Uncompahgre Uplift and vicinity, Grand County, Utah, and Mesa County, Colorado: Geophysical Investigations Map, .

Crabaugh, M., 1993, Entrada Sandstone; an example of a wet aeolian system: Geological Society Special Publications, v. 72, p. 103.

Davatzes, N.C., 2003, Overprinting faulting mechanisms in high porosity sandstones of SE Utah: Journal of Structural Geology, v. 25, p. 1795.

Doelling, Hellmut H., 2001, Map 180 Geologic map of the Moab and eastern part of the San Rafael Desert 30' x 60' quadrangles, Grand and Emery Counties, Utah, and Mesa County, Colorado, 3 pl., 1:100,000, Utah Geological Survey

Eichhubl, P., 2002, Diagenetic sealing of fault-controlled hydrocarbon migration pathways; the Moab Fault, SE Utah, USA: Abstracts of the ...General Meeting of the International Mineralogical Association, v. 18, p. 301.

Garden, I.R., 2001, An exhumed palaeo-hydrocarbon migration fairway in a faulted carrier system, Entrada Sandstone of SE Utah, USA: Geofluids, v. 1, p. 195.

Kaufman, P.S., 2000, Collection and visualization of 3D digital geologic data sets; an example from the Moab fault zone, UT: Annual Meeting Expanded Abstracts - American Association of Petroleum Geologists, v. 2000, p. 76.

Keach, R.W. II, and Purday, N.D.J., 2005, The Role of Visualization in Understanding the Reservoir, Abstract-American Association of Petroleum Geologists (AAPG), National Meeting-Calgary, Canada, Official Program, Vol. 14.

Livaccari, R., 2005, Laramide and Quaternary-age faulting along the northern Uncompahgre Plateau, western Colorado: Abstracts with Programs – Geological Society of America, v. 37, p. 34.

Lucas, S.G., 1997, The Jurassic San Rafael Group, Four Corners region: Guidebook - New Mexico Geological Society, v. 48, p. 115.

Lucas, S.G., 2001, The Middle Jurassic Entrada Sandstone near Gallup, New Mexico; discussion: Mountain Geologist,v. 38, p. 225.

Luedke, R.G., 1994, Measured stratigraphic sections in the Ouray area, western San Juan Mountains, Colorado: Open-File Report - U.S.Geological Survey.

Marfurt, K.J., Kirlin, R.L., Farmer, S.L., and Bahorich, M.S., 1998, 3-D seismic attributes using a semblance based coherency algorithm: Geophysics, v. 63, p. 1150-1165.

Masse, D.J., 1995, 3-D seismic prospecting for Entrada Sandstone reservoirs on the southeastern flank of the San Juan Basin, New Mexico: p. 143.

Milligan, M.R., 2000, Geology of Goblin Valley State Park, Utah: Utah Geological Association Publication, v. 28,p. 421.

Netoff, D., 2002, Seismogenically induced fluidization of Jurassic erg sands, south-central Utah: Sedimentology, v. 49, p. 65.

O'Sullivan, R.B., 1981, Stratigraphic sections of Middle Jurassic Entrada Sandstone and related rocks from Salt Valley to Dewey Bridge in East-central Utah: Oil and Gas Investigations Chart.

O'Sullivan, R.B., 1983, Stratigraphic sections of Middle Jurassic Entrada Sandstone and related rocks from Dewey Bridge, Utah, to Bridgeport, Colorado: Oil and Gas Investigations Chart.

O'Sullivan, R.B., 2000, Correlation of Middle Jurassic San Rafael Group and related rocks from Bluff to Monticello in southeastern Utah: Miscellaneous Field Studies Map - U.S.Geological Survey.

O'Sullivan, R.B., 2003, The Middle Jurassic Entrada Sandstone in northeastern Arizona and adjacent areas: Guidebook - New Mexico Geological Society, v. 54, p. 303.
Otto, E.P., 1973, Depositional environments of Entrada Formation (Jurassic), northeastern Utah: American Association of Petroleum Geologists Bulletin, v. 57, p. 960.

O'Sullivan, R.B., 2004, Correlation of Middle Jurassic San Rafael Group and related rocks from Bridgeport to Ouray in western Colorado: Scientific Investigations Map, 2849 U.S. Dept. of the Interior, U.S. Geological Survey.

Pearson, R.A., 2004, Three-dimensional seismic attributes help define controls on reservoir development; case study from the Red River Formation, Williston Basin: AAPG Memoir, v. 81, p. 43.

Peterson, F., 1974, Correlation of the Curtis, Summerville, and related units (Upper Jurassic) in south-central Utah and north-central Arizona: Abstracts with Programs - Geological Society of America, v. 6, p. 466.

Purday, N.D.J., Keach, R.W. II, and J.P. Sutton, 2004, Total Volume Interpretation: A Holistic Approach to Seismic Structure and Reservoir Characterisation, Proceedings of NAPE/AAPG First West Africa Deepwater Regional Conference Technical Program.

Reese, R.S., 1981, Stratigraphy and petroleum trapping mechanisms of Upper Jurassic Entrada Sandstone, northwestern New Mexico: AAPG Bulletin, v. 65, p. 567.

Reynolds, M.W., and Dolly, E.D., Mesozoic paleogeography of the West-Central United States, Rocky Mountain Paleogeography Symposium, vol.2, 391 pp., 1983
Society of Economic Paleontologists and Mineralogists, Rocky Mountain Section, Denver, CO, United States (USA) 391 pp.

Ridgley, J.L., 1984, Paleogeography and facies distribution of the Todilto Limestone and Pony Express Limestone Member of the Wanakah Formation, Colorado and New Mexico: Abstracts with Programs - Geological Society of America, v. 16, p. 252.

Scott, Robert B., Harding, Anne E., Hood, William C., Cole, Rex D., Livaccari, Richard F., Johnson, James B., Shroba, Ralph R., Dickerson, and Robert P., Geologic Map of Colorado National Monument and Adjacent Areas, Mesa County, Colorado, Geologic Investigations Series I-2740, U.S.Geological Survey, 2001

Sims, W.J., 1995, Possible fault boundary along the northeast side of the ancestral Uncompahgre Uplift, Gunnison County, Colorado: Abstracts with Programs - Geological Society of America, v. 27, p. 55.

Steele, B.A., 1985, Preliminary report on and measured sections of the Middle Jurassic Entrada Sandstone and Wanakah Formation near Placerville, southwestern Colorado: Open-File Report - U.S.Geological Survey, .

Tebo, J.M., 2005, Use of volume-based 3-D seismic attribute analysis to characterize physical-property distribution; a case study to delineate sedimentologic heterogeneity at the Appleton Field, southwestern Alabama, U.S.A: Journal of Sedimentary Research, v. 75, p. 723.

Thomas, W.A., 1996, Contrast in reactivation history of basement faults at the margins of the Uncompahgre Uplift, ancestral Rocky Mountains: Abstracts with Programs - Geological Society of America, v. 28, p. 447.

Tingdahl, K.M., 2005, Semi-automatic detection of faults in 3D seismic data: Geophysical Prospecting, v. 53, p. 533.

Woodward, L.A., 1997, Mesozoic stratigraphic constraints on Laramide right slip on the east side of the Colorado Plateau: Geology Boulder, v. 25, p. 843.

Zhang, F., 2003, Anisotropic semblance analysis and NMO corrections for long-offset data: Exploration Geophysics Melbourne, v. 34, p. 7.